Dalton Transactions

Accepted Manuscript

ROYAL SOCIETY OF CHEMISTRY

www.rsc.org/dalton

Synthesis, characterization and properties of a family of lead(II)-organic frameworks based on a multi-functional ligand 2-amino-4-sulfobenzoic acid exhibiting auxiliary ligand-dependent dehydration-rehydration behaviours

Kou-Lin Zhang,*[a] Zhao-Yin Zhong,[a] Lei Zhang,[a] Chu-Yue Jing,[a] Luke M. Daniels,[b] Richard I. Walton[b]

[a] *College of Chemistry and Chemical Engineering, Yangzhou University, Yangzhou 225002, P.R. China*

[b] *Department of Chemistry, University of Warwick, Coventry, CV4 7AL, UK*

A systematic investigation is reported of the use of the multi-functional ligand 2-amino-4-sulfobenzoate ($asba^{2-}$) to construct lead(II)-organic frameworks in the presence and absence of *N*-donor auxiliary ligands phen, bipy and bix [phen = 1, 10-phenanthroline, bipy = 2, 2'-bipyridine and bix = 1,4-(methylene-benzene)bisimidazole]. Under ambient, aqueous conditions the assembly of $asba^{2-}$ with Pb(II) and phen or bipy leads to two iso-structural 2D double-layer frameworks, $\{[Pb_2(asba)_2(phen)_2(H_2O)]\cdot 2H_2O\}_n$ (**1**) and $\{[Pb_2(asba)_2(bipy)_2(H_2O)]\cdot 2H_2O\}_n$ (**2**). $[Pb_2(asba)_2(bix)_2(H_2O)_2]_n$ (**3**) is obtained in the presence of the auxiliary ligand bix and possesses a 3D network built up from 2D Pb(II)-$asba^{2-}$-bridged double-layer pillared by bix. A 2D (4, 4) topological network $[Pb(asba)(H_2O)]_n$ (**4**) is obtained in the absence of any second ligand or presence of some bistriazole bridging spacers. The coordination modes of the ligand $asba^{2-}$ in **1**-**4** are greatly dependent on the type of the auxiliary ligand and the compounds exhibit

* Corresponding author. Tel./fax: +86 514 87975244. E-mail: klzhang@yzu.edu.cn; koulinzhang2002@yahoo.com

auxiliary ligand-dependent dehydration-rehydration behaviours; **1** shows *in-situ* rapid and reversible dehydration-rehydration behaviour in air, while the iso-structural compound **2** loses crystallinity in air and transforms into $\{[Pb_2(asba)_2(bipy)_2(H_2O)]\cdot H_2O\}_n$ (**2A**) verified by TGA, elemental analysis and powder x-ray diffraction analysis (PXRD). **3** also shows reversible dehydration-rehydration behaviour, but it takes around one week to rehydrate even after exposure to water vapor, while the dehydrated phase of **4** rehydrates to a new crystalline material. **1** and **3** fall within the category of "recoverable collapsing" and "guest-induced re-formation" frameworks. The water molecules in **1** and **3** have some influence on their solid state fluorescent emission intensity.

Introduction

During the past decades, metal−organic frameworks (MOFs) have attracted much interest in supramolecular chemistry, coordination chemistry and materials chemistry, not only because of their intriguing structural and topological novelty, but also owing to their tremendous potential applications in adsorption, microelectronics, ion exchange, separations, nonlinear optics, sensing and heterogeneous catalysis, *etc*.[1−6] However, compared with transition metal MOFs, less attention has been paid to the MOFs of *p*-block metal ions despite their importance in photovoltaic conversion, organic light-emitting diodes, electroluminescence and fluorescent sensors, *etc*.[7] Of these, lead(II)-organic frameworks are of interest for a number of reasons. Pb(II) has the ability to form diverse framework structures with interesting topologies not seen for other metals, due to its large ionic radius, variable coordination numbers, ranging

from 2 to 10, and diverse coordination geometries.[8-9] The coordination geometry of Pb(II) is described as either holodirected or hemidirected. The holodirected geometry is found in Pb(II) complexes with high coordination numbers and can be understood in terms of the crowding effect, while the hemidirected geometry is generally observed in lead(II) compounds with small coordination numbers and is associated with the impact of the stereochemical activity of the $6s^2$ lone pair of Pb(II).[8f] Lead(II)-organic frameworks have been shown to have interesting catalytic activity towards the Knoevenagel condensation reaction[9o] and photophysical properties such as luminescence[10] and birefringence,[11] and may form multi-dimensional Pb-X-Pb (X = O, N, Cl, S) frameworks giving rise to a variety of topologies.[12] The coordination chemistry of Pb(II) in such materials has recently been investigated and frequently discussed in regard to the coordination and stereoactivity of the valence shell lone electron pair in relation to potential uses as functional materials.[13-15]

The structural architectures of MOFs can be varied by changing the metal-ligand ratio, solvents, geometry of the auxiliary ligands, pH and temperature, *etc*.[16] The flexibility of forming various topological structures may be enhanced by using *p*-block metal ions, and in the case of Pb(II), the coordination preference of Pb(II) and its geometry, size and bridging ability of the organic ligands are expected to dictate the final topology of the framework formed.[16c]

The work presented here uses 2-amino-4-sulfobenzoic acid (H_2asba) as the organic ligand precursor (**Chart 1)**. This is based on the following considerations: (1) As a rigid aromatic carboxylate ligand, $asba^{2-}$ can play the role of a bridging rod, so

structural prediction of the resulting polymeric species may be possible to some extent; (2) the acid H_2asba has excellent solubility in water at room temperature, so the interaction between H_2asba and Pb(II) ions can take place easily at close to ambient conditions; (3) the amino functional group is the potential interaction site for forming N-H…O hydrogen bonding or coordinative bonds with the central metal ion; (4) a variety of binding modes of the carboxylate and sulfonate groups are anticipated, which will offer new insights to develop building blocks for the construction of specific coordination arrays; (5) Owing to the presence of aromatic/hetero rings of asba^{2-} and dipyridyl/bisimidazole-type auxiliary ligands in the assembly system, delicate π…π stacking interactions are available to play an important role in the formation of an extended supramolecular network, well known in biological systems.[17] To the best of our knowledge, there are as yet no complexes reported with asba^{2-} as ligand, and indeed the single crystal X-ray structure analysis of H_2asba itself has not been determined.

Herein we describe a systematic study of the preparation, crystallography and properties of a family of four Pb(II) frameworks based on asba^{2-}(**Scheme 1**). $\{[Pb_2(asba)_2(phen)_2(H_2O)]\cdot 2H_2O\}_n$ (**1**) and $\{[Pb_2(asba)_2(bipy)_2(H_2O)]\cdot 2H_2O\}_n$ (**2**) are iso-structural and exhibit a 2D double-layered architecture (phen = 1,10-phenarthrine, bipy = 2,2'-bipyridine). $[Pb_2(asba)_2(bix)_2(H_2O)_2]_n$ (**3**) is a 3D network constructed from 2D Pb(II)-asba^{2-}-bridged double-layers pillared by the auxiliary ligand bix [1,4-(methylene-benzene)bisimidazole]. $[Pb(asba)(H_2O)]_n$ (**4**), a 2D (4, 4)-network, was obtained in the absence of any auxiliary ligands or in the

presence of some bistriazole spacers. The auxiliary ligand-dependent dehydration-rehydration behaviours of **1**-**4** have been studied and solid-state fluorescent properties for all compounds have been studied.

Results and discussion

Synthesis of the complexes

The materials **1-4** were obtained under ambient conditions. An aqueous mixture of lead(II) and H_2asba in the presence/absence of *N*-donor auxiliary ligands typically results in precipitation of a polycrystalline powder directly, but single crystals of **1**-**4** were successfully obtained by keeping the filtrate under ambient air for several days with the addition of NaOH to neutralize the acid. The molar ratio of H_2asba:NaOH was found to be important for the growth of single crystals. Molar ratios of H_2asba:NaOH of 1:2 for **1** and **4**, 1:1 for **2** and **3** were necessary when attempts were made to synthesize **1-4** as single crystals and polycrystalline powder was obtained if other molar ratios were used. It should be mentioned that **2** and **3** can not be obtained without the presence of a small quantity of ethanol and methanol, respectively, to aid the solubility of the ligands bipy and bix. Compound **4** can also be obtained in the presence of some bistriazole bridging spacers [bte = 1, 4-bis(1,2,4-triazol-1-yl)ethane, btp = 1, 3-bis(1,2,4-triazol-1-yl)propane, btb = 1, 4-bis(1,2,4-triazol-1-yl)butane, bth = 1, 6-bis(1,2,4-triazol-1-yl)hexane and bbtz = 1,4-(methylene-benzene)bistriazole], indicating that the coordination ability of these bistriazole bridging auxiliary ligands to Pb(II) is weaker than that of bix and can not compete with the ligand $asba^{2-}$ in this system. All the carboxylate groups of H_2asba in **1**-**4** are found to be deprotonated as

evidenced by FT-IR spectra and the results of crystallographic analysis (vide infra). The ligand asba^{2-} exhibits various coordination modes in **1**-**4** (**Scheme 2**), which exert important influence on the crystalline architectures as described below.

Structure description

{[Pb$_2$(asba)$_2$(phen)$_2$(H$_2$O)]·2H$_2$O}$_n$ (1) and {[Pb$_2$(asba)$_2$(bipy)$_2$(H$_2$O)]·2H$_2$O}$_n$ (2)

1 and **2** are iso-structural and thus we only describe the structure of **1** in detail (**Fig. 1**). The detailed structure of **2** is shown in **Fig. S1**.

The hydrous lead(II) framework **1** crystallizes in the triclinic system with space group *P*-1 (**Table 1**). There are two crystallographically independent hemidirected Pb(II) ions, two asba^{2-} anions, two phen chelating ligands, one coordinated water and two lattice water molecules in the asymmetric unit (**Fig. 1A**). The Pb1 sites are heptacoordinated (**Pb1**O$_5$N$_2$) by two nitrogen atoms from the phen ligand and five oxygen atoms: two from the carboxylate groups, two from the sulfonate groups of two asba^{2-} ligands and one from the coordinated water. Pb2 is hexa-coordinated (**Pb2**O$_4$N$_2$) with two nitrogen atoms (N4, N5) from another phen, two oxygen atoms (O11, O12) from the chelating carboxylate group and two sulfonate oxygen atoms (O7, O10) from two asba^{2-} ligands. The bond distances in the carboxylate group [(1.205(3)-1.317(3) Å] of H$_2$asba (see supplementary cif for H$_2$asba·H$_2$O, also obtained in this work) clearly show some difference between single- and double-bond character, while almost identical bond lengths in the carboxylate group in **1** [1.265(11)-1.284(10) Å] are observed and consistent with delocalization as a result of the coordination of the carboxylate group to Pb(II).

It is useful to compare our new materials with previous frameworks that include Pb(II).[8f,18] The Pb-N bond distances for lead(II) complexes with an inactive $6s^2$ lone pair usually fall in the range of 2.62-2.88 Å[19] and the Pb-N distances [2.497 (7) - 2.623(8) Å] in **1** fall within the ranges usually observed in Pb(II) complexes containing a phen ligand with an active $6s^2$ lone pair.[8b,9c] Furthermore, the distances of Pb-$O_{sulfonate}$ and Pb-O_{water} are longer than those of Pb-$O_{carboxylate}$ (**Table 2**). Therefore, the presence of an active $6s^2$ lone pair opposite to Pb-$O_{carboxylate}$ and near to Pb-$O_{sulfonate}$ is deduced. So, both Pb1 and Pb2 exhibit hemidirected geometry with the (**Pb1**N_2O_5) and (**Pb2**N_2O_4) chromophores, respectively (**Fig**. **1A**).

One $asba^{2-}$ anion acts as a tridentate ligand in η^1:η^1:η^1:μ_2- coordination mode (**Scheme 2**): the carboxylate group (O1C13O2) exhibits chelating coordination and the sulfonate group (S2O5O7O13) shows monodentate coordination. The other $asba^{2-}$ anion acts as a pentadentate ligand with η^1:η^1:η^1:η^1:η^1:μ_4- coordination mode: the carboxylate group (O11C13O2) also exhibits chelating coordination while the sulfonate group (S1O8O9O10) exhibits the tridentate coordination, linking three lead(II) atoms. These two $asba^{2-}$ anions coordinate with the lead(II) ion alternatively, as a result, a 26-membered macrometalcyclic ring is formed. Furthermore, the tridentate sulfonate group (S1O8O9O10) and its symmetric equivalent (S1aO8aO9aO10a) coordinate with two symmetric Pb1 atoms, resulting in the centrosymmetrical sulfonate-bridged dinuclear eight-membered (Pb1O8S1O9Pb1aO8aS1aO9a) secondary building unit (SBU) [$Pb_2(SO_3)_2(phen)_2$], which further links the adjacent macrometalcyclic ring into 1D necklace-like double

chain (**Fig. 1B**). Within the double chain, the π···π stacking interactions exist between the phen ligands or between the benzene ring of asba^{2-} and aromatic ring of phen (centeroid-centeroid: 3.675, 3.754 Å). 1D necklace-like double chains are further linked with each other by such SBUs along [100] direction, as a result, a 2D double-layered framework is formed along [110] plane (**Fig. 1C**).

Hydrogen bonds exist extensively in the structure of **1** (**Table 3**). The coordinated water O1W together with the lattice water O2W and O3W form hydrogen-bonded trimers with average Ow···Ow distances of 2.863 Å which matches well the expected distance of hydrogen bonds between water molecules.[20] Interlayer π···π stacking interactions exist between the phen ligands (centeroid-centeroid: 4.030 Å). A 3D supramolecular network is thus formed through such weak interactions (**Fig. 1E**).

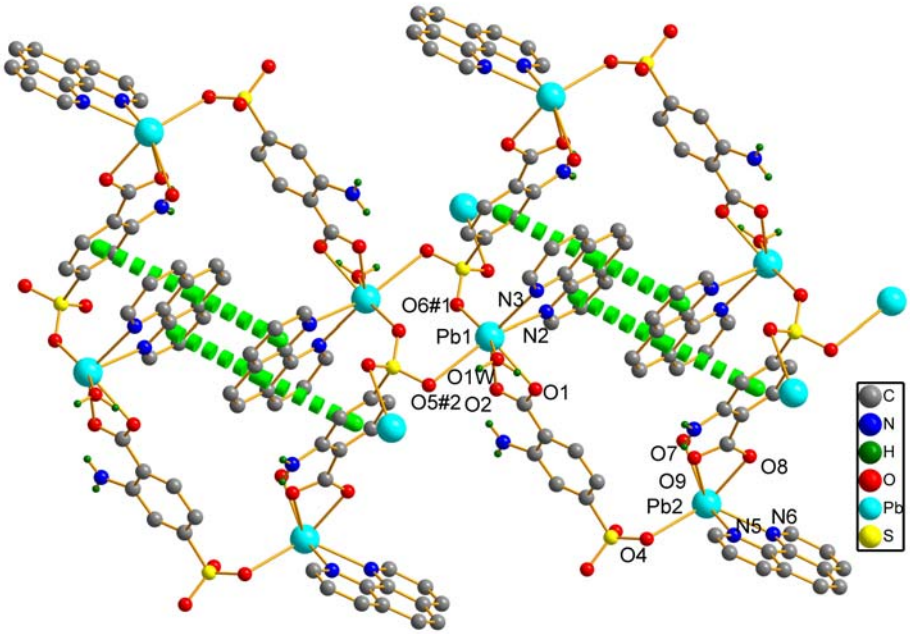

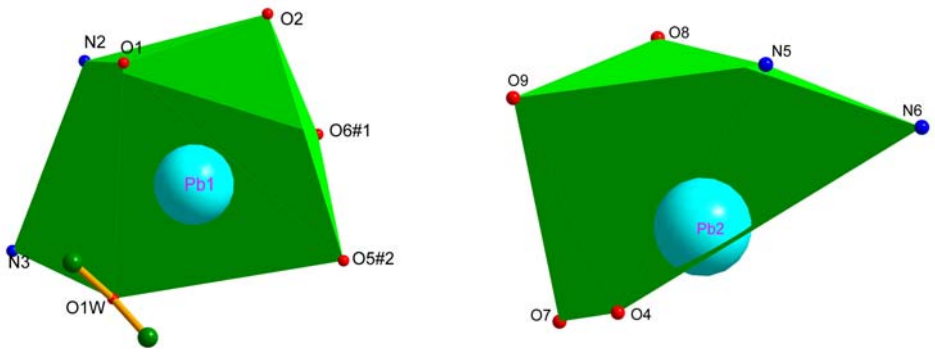

A

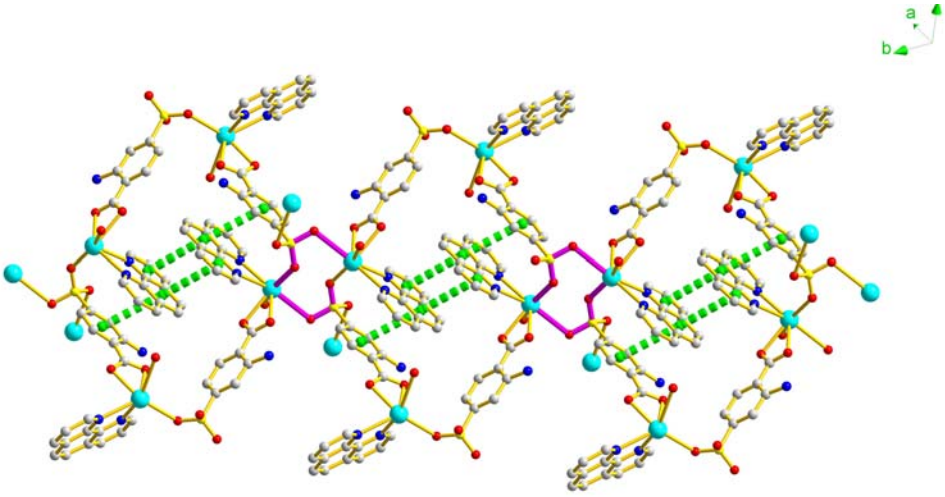

B

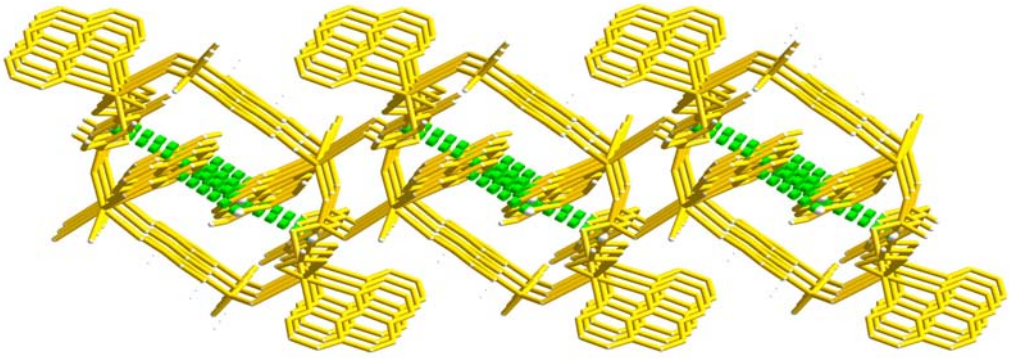

C

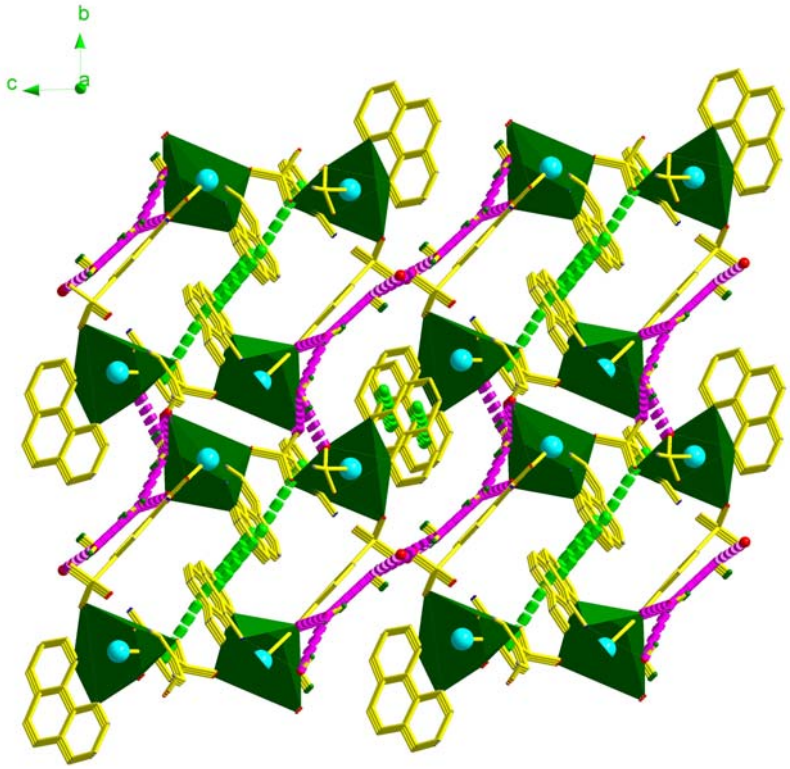

D

Fig. 1 A Top: View of the coordination environment of the Pb(II), the coordination mode of the asba^{2-} ligand and the centrosymmetrical dinuclear SBU in **1**. #1 x-1 y-1 z-1 #2 x-1 y-1 z.

Bottom: Polyhedral representation of the hemidirected Pb1 and Pb2.

B The 26-membered uncoplanar metallamacrocycle: metallacalix[4]arene were linked by the SBU,resulting the formation of 1D necklace-like double chain, showing the π···π stacking interactions within the double chain.

C 2D double-layered framework.

D 3D supramolecular network formed through interlayer hydrogen bonds (pink dashed lines) and π···π stacking interactions (green dashed lines).

$[Pb_2(asba)_2(bix)_2(H_2O)_2]_n$ (3)

3 crystallizes in the triclinic system with space group *P*-1. In the asymmetric unit, there are two crystallagraphically independent lead(II) ions, two independent asba^{2-} ligands, two bix and two coordinated water molecules. The Pb1 is penta-coordinated (**Pb1**O_4N) by one nitrogen atom (N5) from the bix ligand and four oxygen atoms: one sulfonate oxygen atom O8 from one asba^{2-} ligand and two carboxylate oxygen atoms

(O6, O7) from one asba^{2-} ligand and one coordinated water O2W with the Pb1-O distances ranging from 2.427(6) to 2.947(6) Å and the Pb1-N5 distance being the shortest [2.422(7) Å], indicating that Pb1 exhibits hemidirected geometry and the 6s^2 active lone pair lies opposite to the bond Pb1-N5 and near the bond Pb1-O10. Pb2 is heptacoordinated (**Pb2**O_6N) with one nitrogen atom (N2) from the other bix ligand, two oxygen atoms (O4, O5) from the chelating carboxylate group and two sulfonate oxygen atoms (O1, O2) from two different asba^{2-} ligands with Pb2-O distances ranging from 2.468(6) to 2.954(7) Å to furnish a hemidirected geometry and the 6s^2 lone pair lies opposite to the Pb2-N2 bond [2.465(6) Å] (**Fig**. **2A**).[8f]

The overall 3D architecture of **3** can be described as follows. The carboxylate group of one asba^{2-} chelates with the Pb2 atom while the sulfonate group coordinates with Pb2 through Pb2–O2 bond, leading to the formation of 1D asba^{2-}-bridged linear chains which are further pillared alternatively by bix in *TT* (*trans-trans)* conformation and *zigzag* asba^{2-}-Pb1-bix-Pb1-asba^{2-}- units in which the asba^{2-} ligand exhibits the η^1:η^1:η^1:η^1:μ_3- coordination mode (**Scheme 2**). As a result, a 2D network with point symbol $(8^2)(4^2.8^2)$ is formed.[16a] There are two macrometalcyclic rings: uncoplanar metallacalix[8]arene and metallacalix[4]arene within the 2D network (**Fig**. **2B**). The adjacent 2D layers were further linked each other by the bonds Pb1-O8 [2.947(6) Å] and Pb2-O1 [2.957(7) Å], resulting in a 3D pillared-layered architecture in which 2D Pb(II)-asba^{2-}-bridged double-layer are pillared by bix (**Fig**. **2C**).

Hydrogen bonds exist extensively in the lattice of **3** between the coordinated water molecules and the oxygen atoms of both carboxylate (O5...O1W 2.833 Å, O7...O2W

2.766 Å) and sulfonate groups (O3...O1W 2.770 and O9...O2W 2.720 Å) of the asba^{2-} ligand with an average O-H...O hydrogen bond distance of 2.758 Å, which further stabilize the 3D framework.

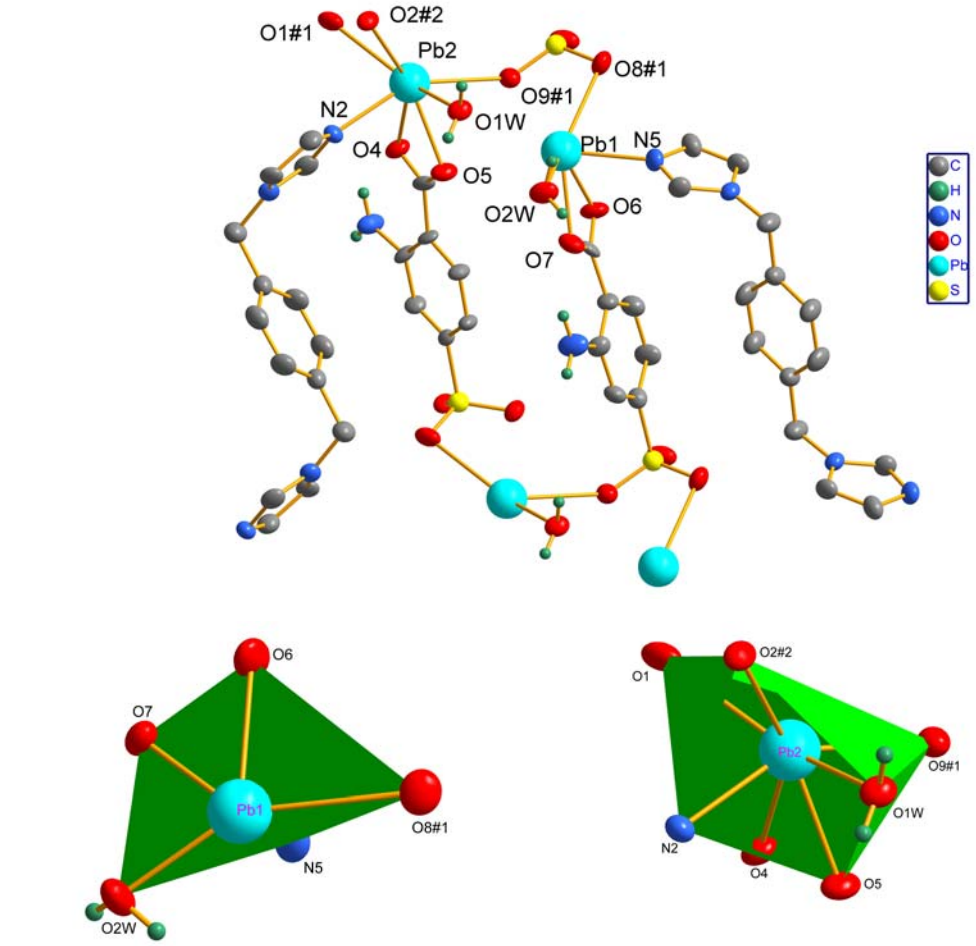

A

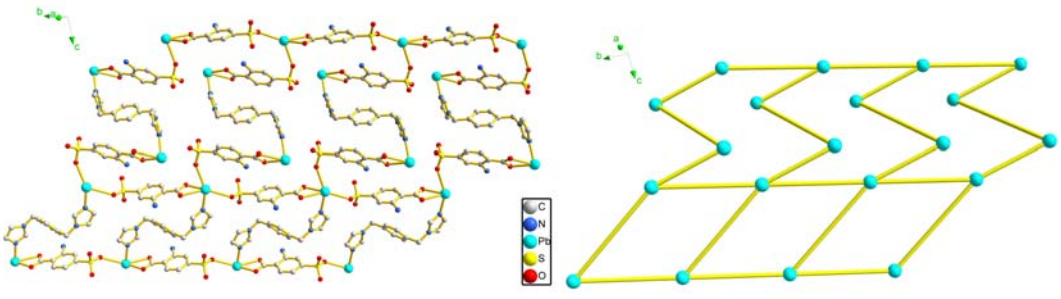

B

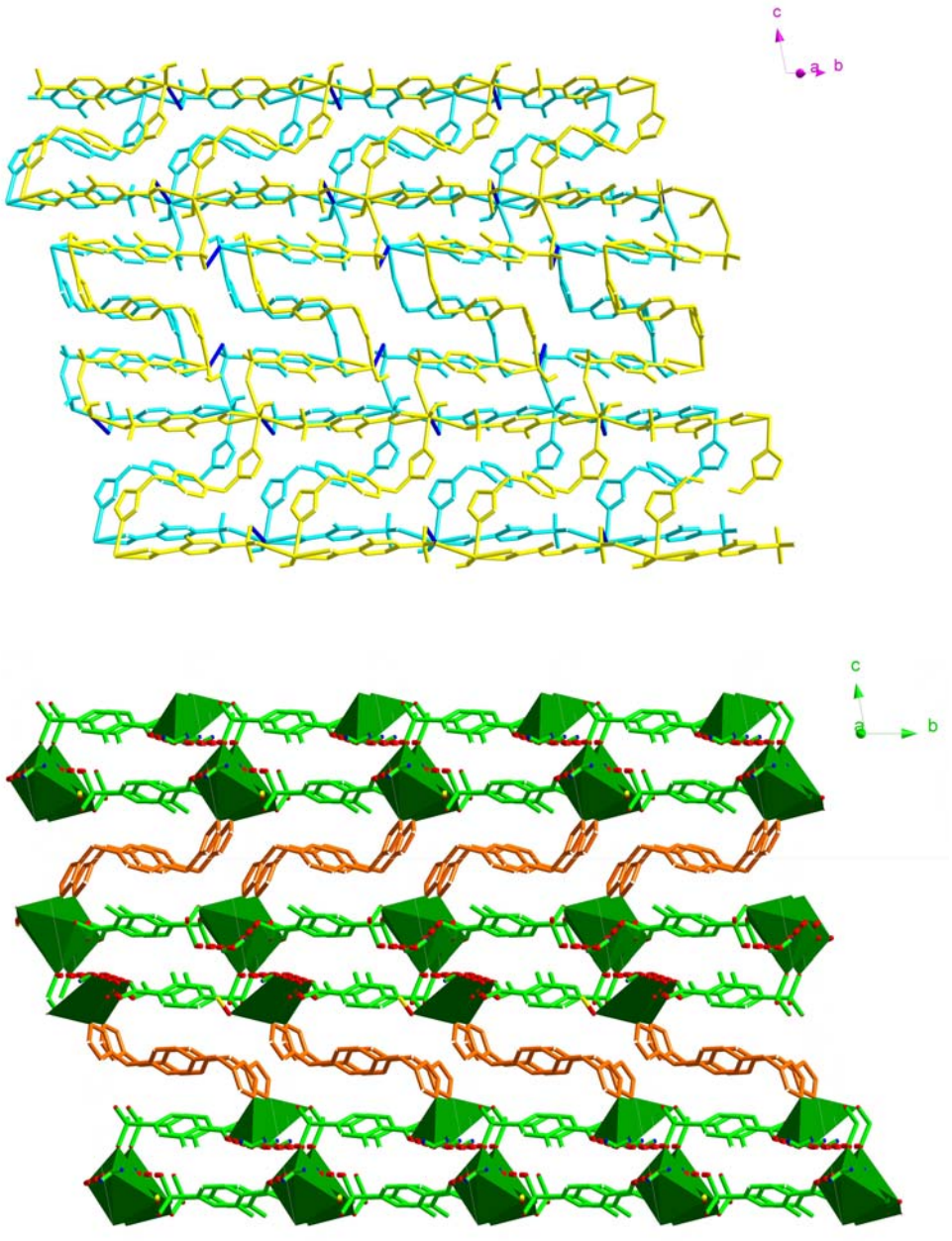

C

Fig. 2 A Top: View of the coordination environment of the Pb(II) atoms, the coordination mode of the asba^{2-} ligand in **3**. # 1 -x, 1-y, z #2 x-1, y-1, z.

Bottom: Polyhedral representation of the hemidirected Pb1 and Pb2.

B 2D $(8^2)(4^2.8^2)$ topological network with two kinds of uncoplanar metallamacrocyclic ring: metallacalix[8]arene and metallacalix[4]arene.

C Top: The adjacent 2D layers were linked by the covalent bonds Pb1-O8 and Pb2-O1 (blue lines) into 3D network.

Bottom: Polyhedral representation of the final 3D framework in which 2D Pb(II)-asba^{2-}-bridged double-layer were pillared by bix. (Hydrogen bonds: pink dashed lines).

[Pb(asba)(H_2O)]$_n$ (4)

4 crystallizes in the monoclinic system with space group $P2_1/c$. In the asymmetric unit, there is one crystallographic independent lead(II), one asba^{2-} and one coordinated water molecule. The lead(II) atom is hexacoordinated by one nitrogen atom (N1) from one asba^{2-} ligand and five oxygen atoms, among which two carboxylate oxygen atoms (O4, O5) from one asba^{2-} ligand and two sulfonate oxygen atoms (O2, O3) from two asba^{2-} ligands and one oxygen atom (O1W) from water molecule to furnish a hemidirected [**Pb**N_1O_5] geometry (**Fig. 3A**). The sulfonate group coordinates with the lead(II) ion in *syn-syn* coordination mode, resulting in an eight-membered S1O2O3PbS1O2aO3aPba secondary building unit (SBU) [$Pb_2(SO_3)_2$] and these are further linked by the asba^{2-} bridge, leading to the formation of 1D double-chains (**Fig. 3B**) further linked each other through the Pb-N bonds, as a result, a 2D network is formed (**Fig. 3C**), in which the asba^{2-} ligand exhibits η^1:η^1:η^1:η^1:η^1:μ_4- coordination mode (**Scheme 2**).

If pseudo atoms are placed in the centre of the SBUs, which are then further treated as a nodes, with the distances between the pseudo atoms as linkers (8.7993 and 9.7183 Å), then the net can be simplified as a 2D (4, 4) topological net.[1k]

The interlayer hydrogen bonds between the coordinated water molecules and both coordinated and uncoordinated sulfonate oxygen atoms [O1, O3] further extend the 2D layer in "ABAB" packing mode into a 3D supramolecular network [O1W - H1WA … O1 2.771(5); O1W - H1WB … O3 2.949(5) Å] (**Fig. 3D**).

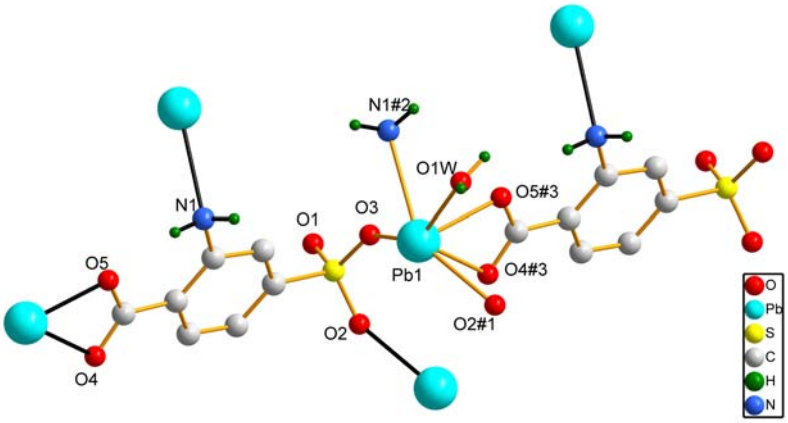

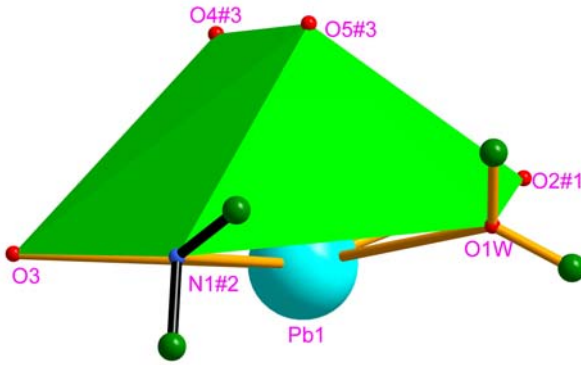

A

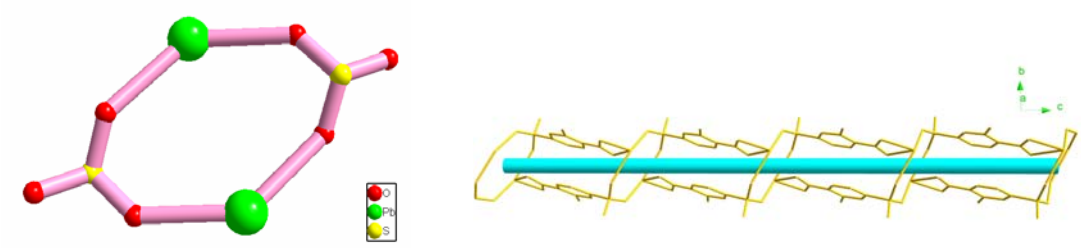

B

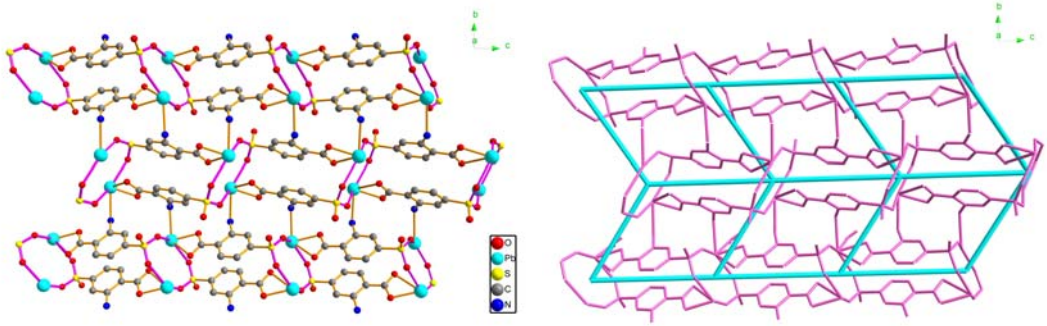

C

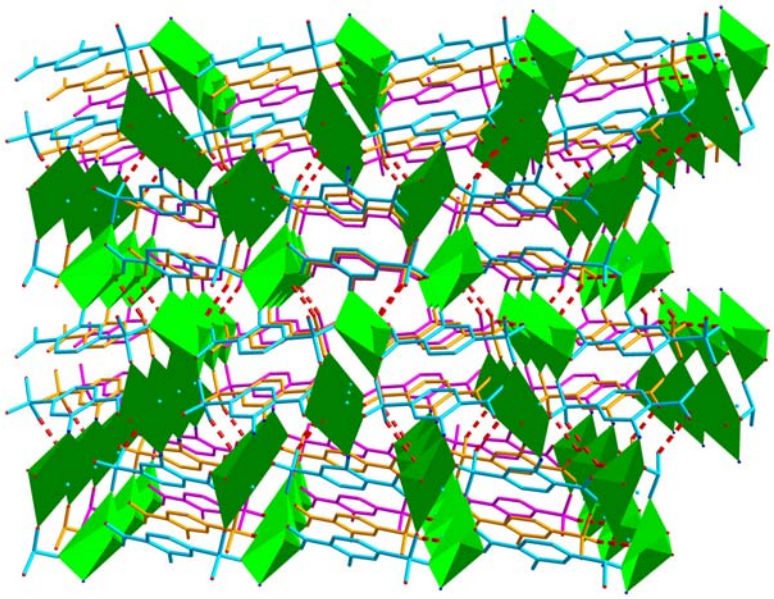

D

Fig. 3 A Top: The diagram showing the coordination geometry of the Pb(II) ion in **4.** Symmetry transformations: #1: -x+3/2, y-1/2, z-1/2 #2: x, 1/2-y, 1/2+z #3: x, y, 1+z.
Bottom: Polyhedral representation of the hemidirected Pb(II).
B View of the $[Pb_2(SO_3)_2]$ SBU and 1D $asba^{2-}$-bridged double chain with 2_1 rotation axis.
C View of 2D network formed through the 1D double chains linked by Pb-N bonds and schematic representation of the 2D (4,4) topological network.
D: 3D supramolecular network formed through the interlayer hydrogen bonds (pink dashed lines).

FT-IR spectra and thermal stability

The FT-IR spectral data show features attributable to the carboxylate stretching vibrations of **1**, **2A**, **3** and **4**. The absence of bands in the range of 1680-1760 cm^{-1} indicates the complete deprotonation of H_2asba in these four compounds. The characteristic bands of the carboxylate groups appear in the range 1613-1649 cm^{-1} for the asymmetric stretching and 1384-1490 cm^{-1} for the symmetric stretching. The characteristic stretching vibrations for the sulfonate group in **1**, **2A**, **3** and **4** are seen at 1200, 1211, 1250 and 1200 cm^{-1}, respectively. The broad band centered at 3400 cm^{-1} corresponds to the mixed vibrations of both H_2O and $–NH_2$ in **1**, **2A**, **3** and **4**.[21]

To study the thermal stability of the compounds, thermogravimetric analysis (TGA) was performed under flowing N_2 with a heating rate of 10 °C·min^{-1} (**Fig. 4**). The TGA curve of **1**, shows a gradual weight decrease of 3.86 % from 100 to 120 °C that corresponds to the loss of one coordinated and two lattice water molecules (calcd: 4.29 %). A sharp weight loss beginning at 350 °C indicates decomposition of the framework.

The weight loss of 2.39 % from 234 to 273 ˚C corresponds to the release of one coordinated and one lattice water molecule, which further reveals that the formula of the partly dehydrated phase of $\{[Pb_2(asba)_2(bipy)_2(H_2O)]\cdot 2H_2O\}_n$ (**2**) is $\{[Pb_2(asba)_2(bipy)_2(H_2O)]\cdot H_2O\}_n$ (**2A**) (calcd. 3.02 %). The second step begins from 351 ˚C and the whole decomposition process is incomplete at 800 ˚C. Powder X-ray diffraction further shows that the structure of **2A** is different from that of **2** (**Fig. 5**).

For **3**, the first step weight loss of 3.22 % (calcd. 3.40 %) in the temperature range 114 to 215 °C corresponds to the removal of two coordinated water molecules. A sharp weight loss beginning at 354 ˚C indicates the decomposition of the framework.

The TGA of **4** exhibits two main steps of weight loss. A weight loss of 4.66 % in the temperature range 228 – 260 ˚C is in agreement with the release of the coordinated water molecules (calcd: 4.09 %). The second step of weight loss from 390 ˚C corresponds to the combustion of the organic groups.

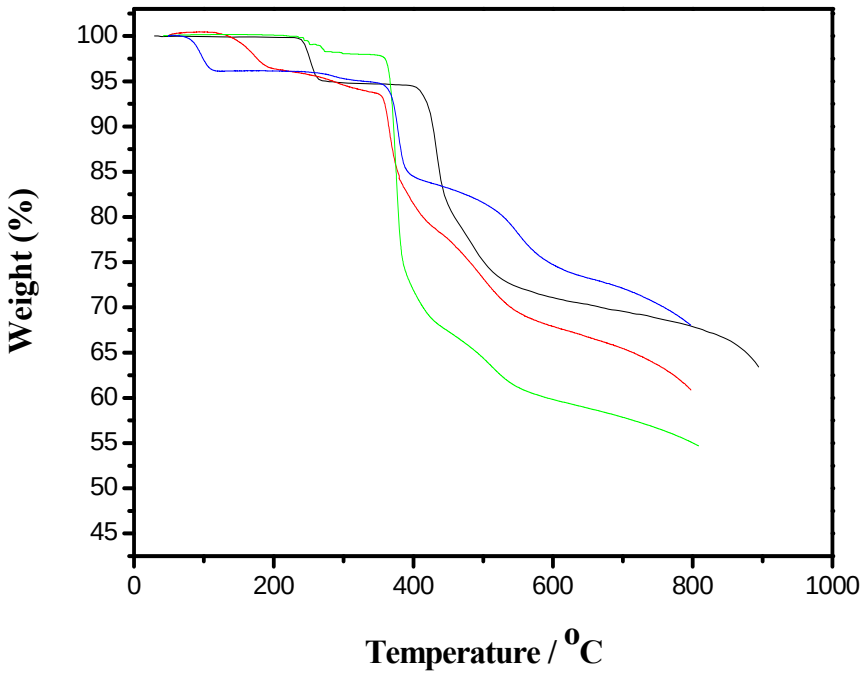

Fig. 4 TGA curves of **1** (blue), **2A** (green), **3** (red) and **4** (black).

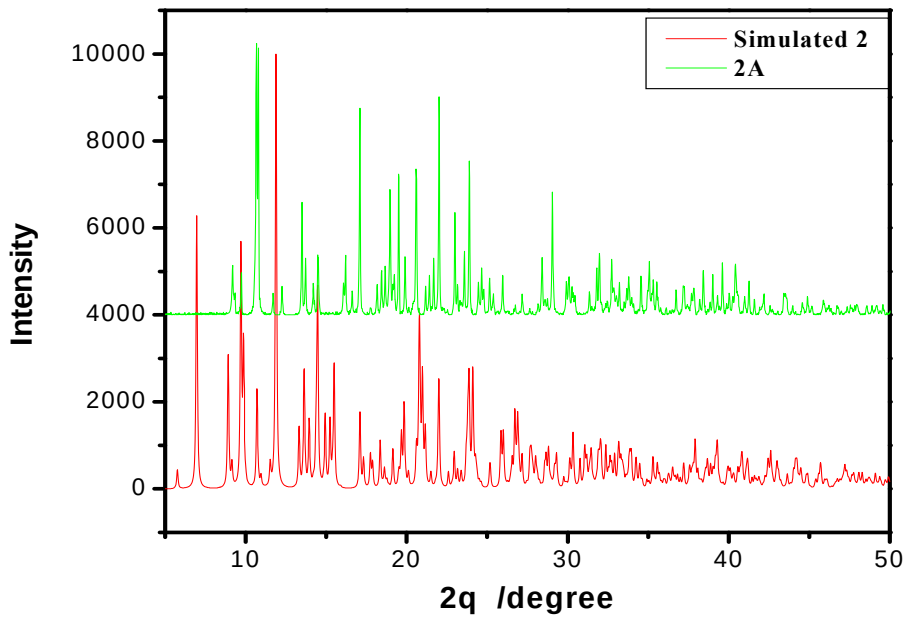

Fig. 5 PXRD patterns**:** (red) simulated from the single-crystal data of **2** with Mercury 1.4.2., (green) for the powder sample **2A**.

Dehydration-rehydration behaviours of 1, 3 and 4

Thermogravimetric analysis (TGA) shows clearly that both the interstitial and coordinated water molecules in **1**, **3** and **4** could be removed upon heating. To study the dehydration-rehydration properties of **1**, **3** and **4**, *in situ* variable temperature powder X-ray diffraction analysis (VT-PXRD) was performed in the static air over the temperature ranges 30-120-30 ℃ for **1** (**Fig. 6**), r.t.-215 ℃-r.t. for **3** (**Fig. 7**) and r.t.-260 ℃-r.t. (r.t. = room temperature) for **4** (**Fig. 8**), respectively. It should be pointed out that the dehydrated phases of **1**, **3** and **4** retain crystallinity after the loss of water molecules, but the structures of the desolvated materials are changed, as supported by the *in situ* VT-PXRD patterns at 120 °C for **1**, 215 ℃ for **3** and 260 ℃ for **4**, respectively. Remarkably, the VT-PXRD patterns clearly show that the dehydrated phase of **1** rehydrates rapidly in the air, resulting in the re-establishment of the original structure. So, **1** undergoes *in situ* rapid and reversible dehydration-rehydration behaviour just in the static air. In order to study the stability of the dehydrated phase of **1** and determine if the reverse structural transformation can occur just on cooling, we measured XRD data under dry nitrogen. –The water is removed at a slightly lower temperature and then on cooling the phase remains dehydrated (**Fig. 6B**). This proves that the water is removed and the dehydrated phase is stable in the absence of atmospheric water.

It should be noted that it takes about one week for the dehydrated phase of **3** to absorb the water molecules and revert to the original structure even in the presence of water vapor.

The reversible dehydration-rehydration behaviours of **1** and **3** are further verified

by the TGA analysis of the rehydrated materials of **1** and **3**. The first step mass loss corresponding to water molecules in TGA of the rehydrated materials is 4.23 % (calcd: 4.29 %) for **1** and 2.83 % (calcd. 3.40 %) for **3**, respectively (see **Fig. S2**), showing that complete rehydration had been achieved.

4 shows quite different dehydration-rehydration behaviour from **1** and **3**: the dehydrated phase of **4** rehydrates to a new crystalline phase whose structure is different from the original structure, verified by the different PXRD pattern compared with those of both the original bulk sample and the simulated ones (**Fig. 8**). So, this dehydration of **4** is irreversible.

The framework integrity of **1** and **3** can be maintained after a number of desorption-adsorption cycles, which indicates that these two compounds may possibly have potential use as water adsorbents.

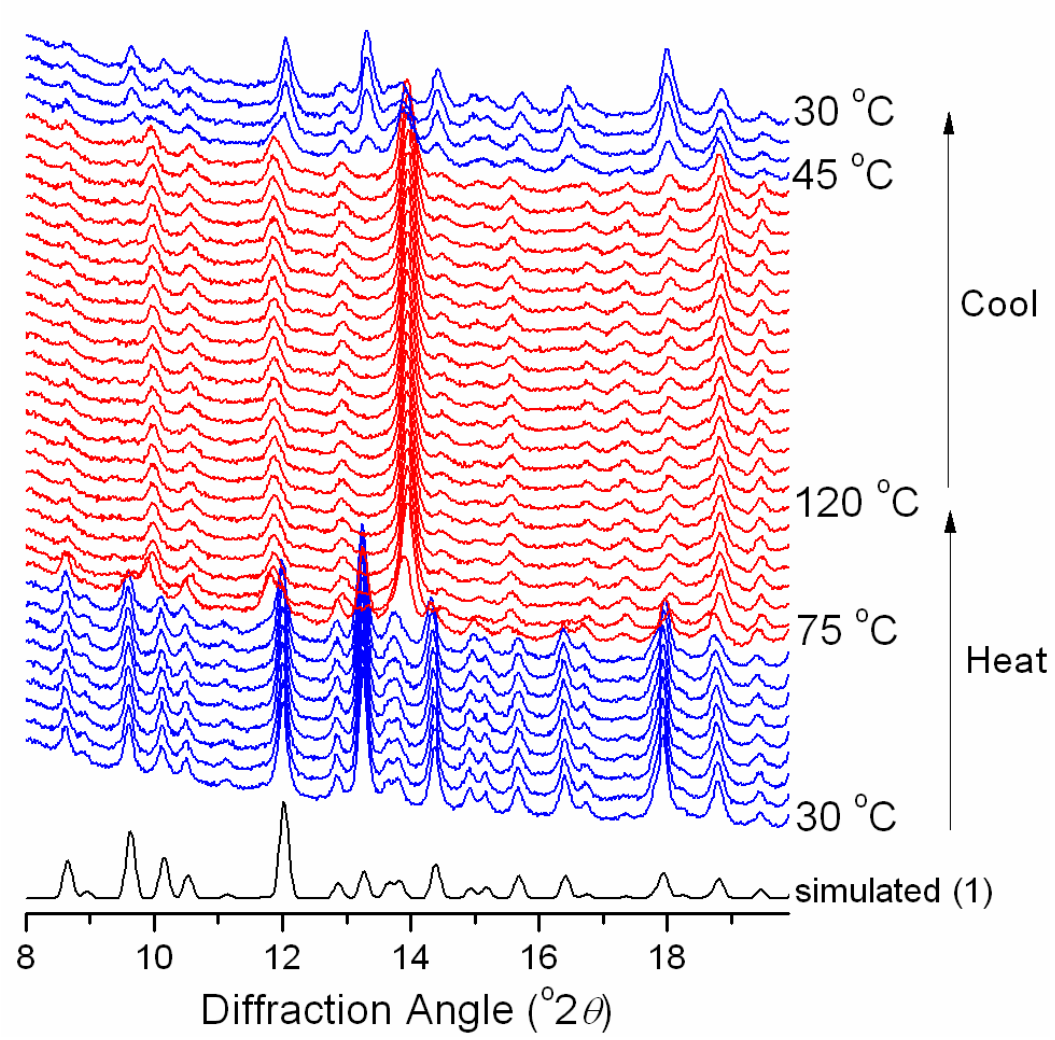

Fig. 6 VT-XRPD patterns recorded during the heating of **1** showing the complete departure of the water molecules at 120 °C (red line) for **1**, leading to a new dehydrated phase which further shows rapid *in situ* reversible dehydration-rehydration just in static air.

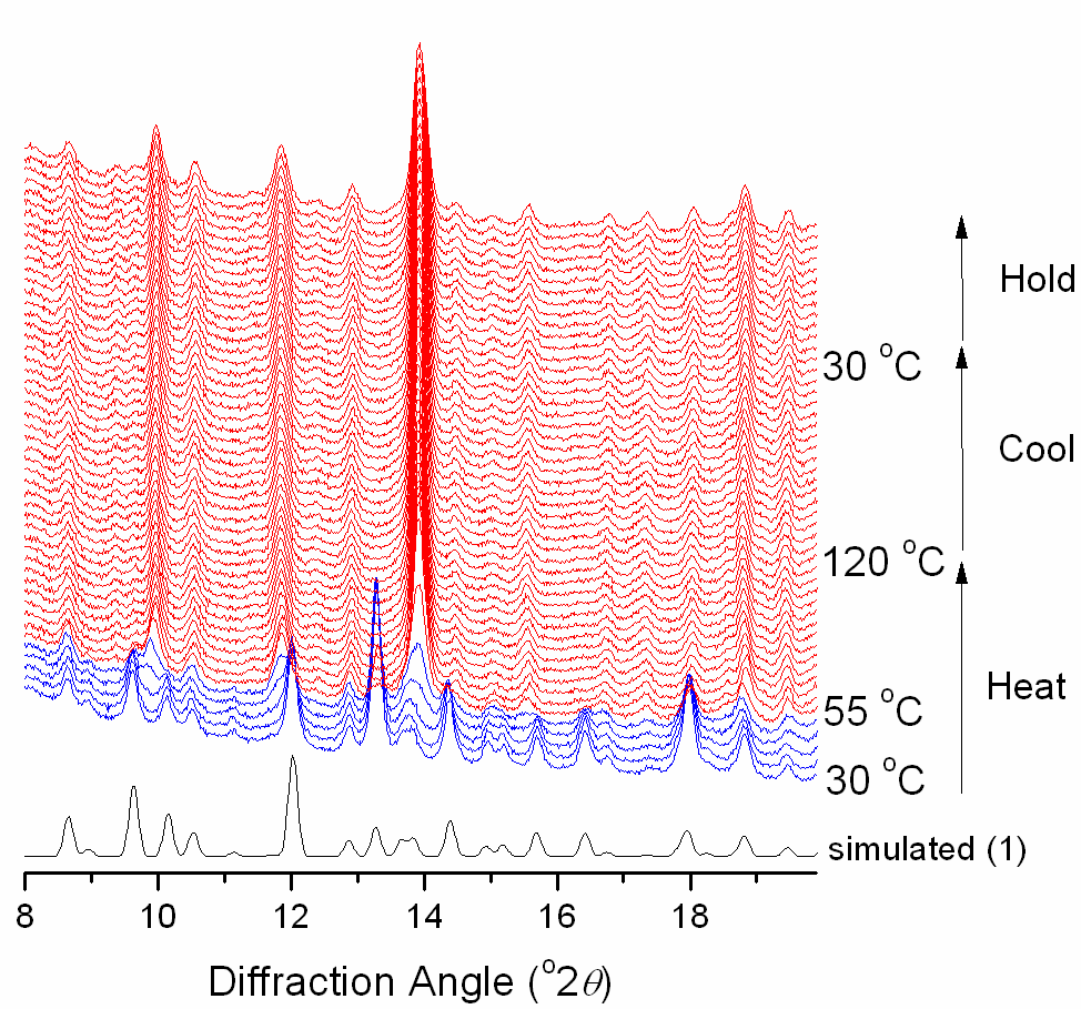

Fig. 6B VT-XRPD patterns recorded during the heating of **1** in dry nitrogen atmosphere showing the complete departure of the water molecules at 120 °C (red line) for **1**, leading to a new dehydrated phase which on cooling remains dehydrated.

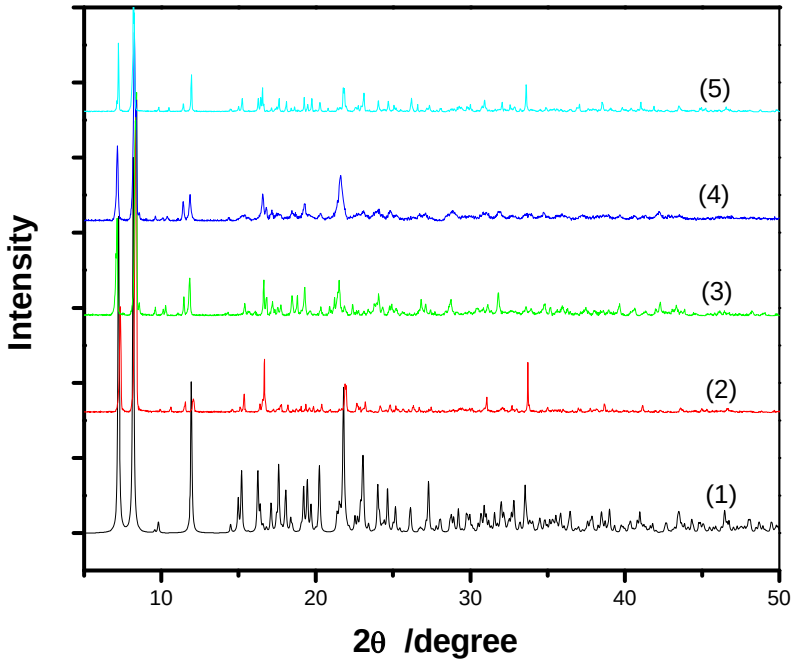

Fig. 7 XRPD patterns for **3**: (1) the simulated XRD pattern calculated from single-crystal data of **3** with Mercury 1.4.2.; (2) as-synthesized **3** measured at room temperature, (3) after removal of the water molecules at 215 ºC; (4) after exposure of the dehydrated material of **3** to water vapor at room temperature for two days; (5) after exposure of the dehydrated material of **3** to water vapor at room temperature for one week.

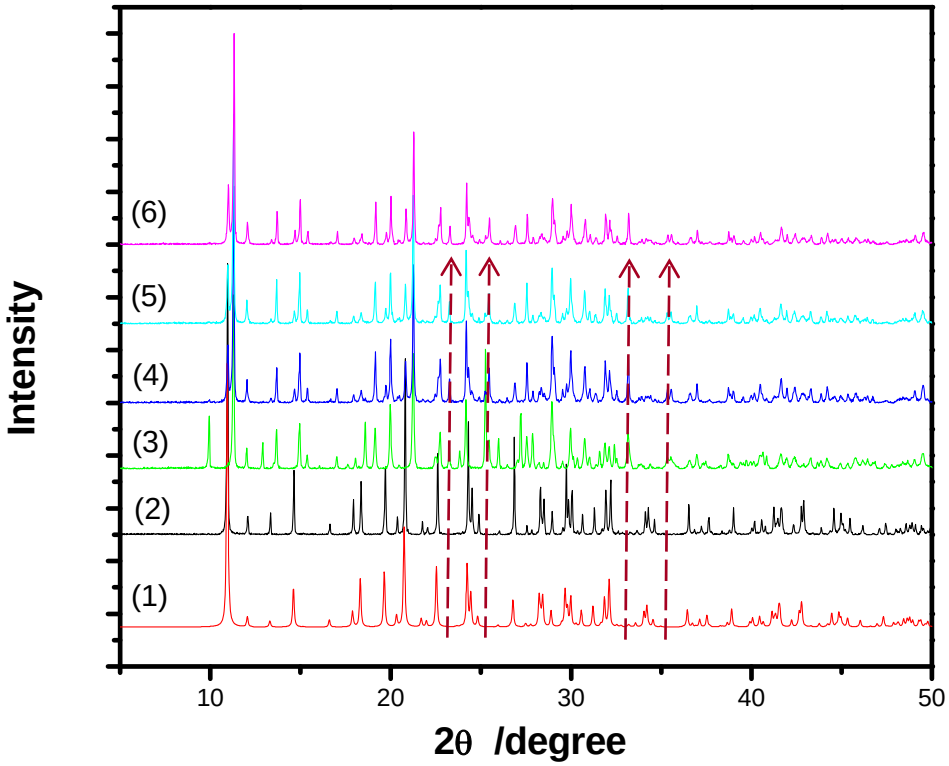

Fig. 8 XRPD patterns for **4**: (1) the simulated XRPD pattern calculated from single-crystal data of **4** with Mercury 1.4.2.; (2) as-synthesized **4** measured at room temperature; (3) after removal of the water molecules at 260 ºC; (4) after *in-situ* introduction of the water molecules in the static air into the desolvated material at room temperature; (5) after exposure of the dehydrated material of **4** to water vapor for two weeks and (6) for one month at room temperature. (The dashed lines are used to denote the positions of some new peaks appearing in the rehydrated material of **4**).

Desorption/adsorption to gases

In order to test the ability of all the dehydrated materials to host molecules other than water, several sorption experiments were carried out. We considered molecules that exhibit current interest for storage, for example, carbon dioxide (CO_2) and nitrogen (N_2). Further, gas sorptions were performed at 278 K to give more reliable results related to crystal structures determined at room temperature. The dehydrated materials of **1**, **2A**, **3** and **4** show almost no uptake capacity to N_2 molecules at 278 K. Only the

dehydrated material of **1** showed weak adsorption capacity in CO_2 uptake with a final uptake of 10 $mg.g^{-1}$ (1.0 wt %) at 38 atm. (**Fig. 9**), the other three materials show almost no adsorption to CO_2. The adsorption of CO_2 by **1** may be attributed to the fact among the materials we have studied it contains the largest conjugated delocalization system phen, which may strengthen the electric interaction between the guest small molecules and host framework. Furthermore, it should be noted that the dehydrated **1** showed selective uptake of CO_2 over N_2 at 278 K, which may be attributed to the smaller kinetic diameter of CO_2 compared to that of N_2 (CO_2, 3.3; N_2, 3.6 Å) and the significant quadrupole moment of CO_2 (-1.4×10^{-39} cm^2), which generates specific interactions with the host framework.[1j, 22]

To determine if the adsorption of CO_2 by **1** is reversible, in situ XRD patterns were measured under a flow of pure CO_2 at atmospheric pressure. First, we note that addition of CO_2 to the hydrated phase gave no change in the powder XRD patterns. However, addition of CO_2 to the dehydrated phase of **1** resulted in an increase in the background of the pattern immediately. This is reversible if N_2 is then added, and then repeatable upon switching back to CO_2 (**Fig. S3**). The Bragg peaks remain in the same place, suggesting the framework of the structure is unaffected by addition of gas. Our conclusion is that the CO_2 is taken up by the solid in a disorderd way at ambient pressure so gives diffuse scattering that is responsible for the increased background of the patterns.

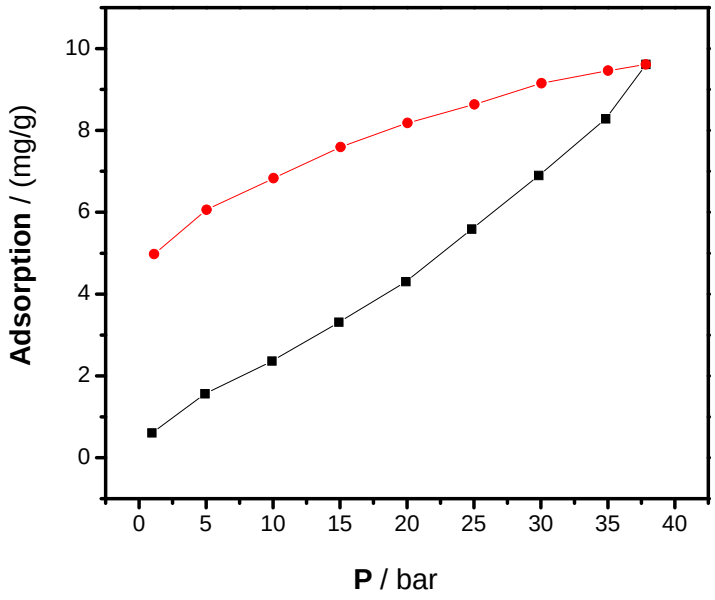

Fig. 9 Sorption isotherm of CO_2 measured at 278 K for **1** (black: adsorption, red: desorption).

Fluorescent properties

To compare the relative fluorescent intensities of the materials **1**, **2A**, **3** and **4** we measured the emission spectra of all the complexes and free acid with the same excitation wavelength (**Fig**. **10**). The free acid H_2asba exhibits a maximum fluorescent emission at 502 nm upon excitation at λ_{ex} = 300 nm. Excitation of the microcrystalline samples **1**, **2A**, **3** and **4** also at λ_{ex} = 300 nm leads to the generation of similar blue-shifted fluorescent emissions for **1**, **2A** and **4** with the maximum emission centered around 472 nm, indicating the auxiliary ligands bipy and phen almost have no influence on the emission mechanism since the free ligands bipy and phen show the maximum emission at 400 and 392 nm (λ_{ex} = 300 nm), respectively (see **Fig**. **S4**). So the blue shifts for **1**, **2A** and **4** are likely caused by the coordination of the multi-functional ligand 2-amino-5-sulfobenzoate perturbed by the lead(II) ion.[8b,23] An

even more blue-shifted emission with the maximum emission peak around 436 nm was observed in **3**, which indicates that the auxiliary flexible bridging ligand bix has great influence on the positions and strengths of fluorescent emission. Such a large blue shift may likely be caused by the coordination of $asba^{2-}$ and an interaction between ligands perturbed by Pb(II).[8b,23] The maximum emission intensity of **2A** among the four compounds may be attributed to the fact that **2A** contains the least content of water molecules (calcd. 3.02 %). It should be noted that, after removal of the water molecules, the maximum emissions of the dehydrated materials of **1** and **3** (**Fig**. **S5-S6**) become stronger than those of the corresponding hydrated materials **1** and **3**, indicating that the water molecules in **1** and **3** have some influence on their fluorescent intensity.

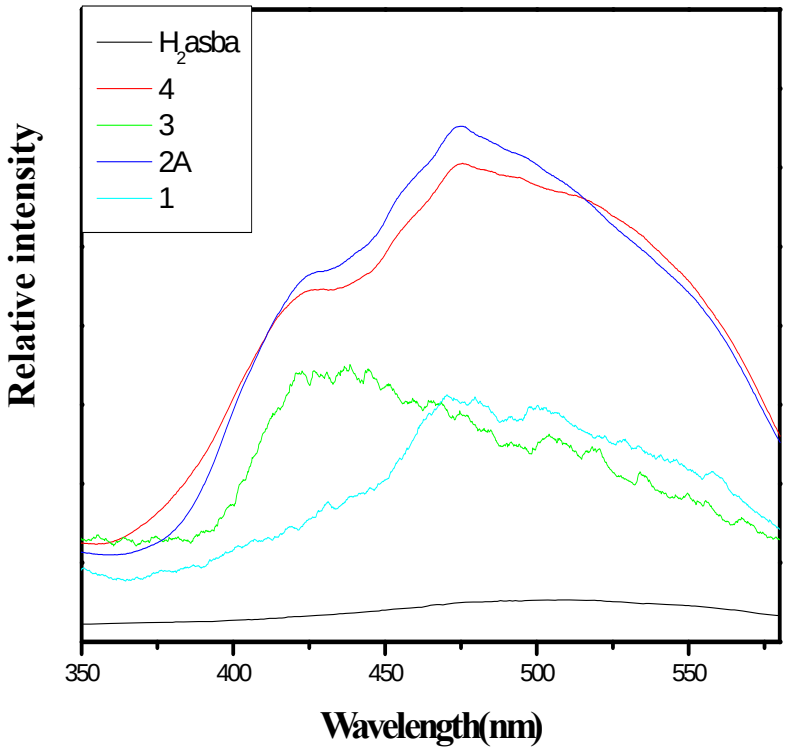

Fig. 10 Solid state fluorescent spectra for **1**(cyan), **2A**(blue), **3**(red), **4**(red) and H_2asba (black) (λ_{ex} = 300 nm).

Conclusion

In summary, the present study shows that the ligand asba^{2-} and Pb(II) ion can act as convenient building blocks for the construction of MOFs with interesting properties. In this way, the first examples of a family of four lead(II) MOFs with H_2asba were generated, their structures being greatly dependent on the type of used auxiliary ligand (or its absence). **1** and **2**, exhibiting isostructural 2D double-layered frameworks, are formed in the presence of auxiliary chelating ligands phen and bipy, respectively. In the case of using the auxiliary flexible ligand bix, a novel 3D pillared-layered framework **3** was obtained successfully. **4**, a 2D (4, 4) topological network, is formed in the absence of any auxiliary ligands or in the presence of some bis(triazole) bridging spacers. The most interesting property of **1** is its *in situ* rapid and reversible dehydration-rehydration behaviour simply in air, while the isostructural compound **2** loses crystallinility under the same conditions. **1** and **3** show guest-induced structural recovery, which falls within the category of "recoverable collapsing" and "guest-induced re-formation" framework materials, while **4** shows irreversible dehydration-rehydration behaviour and rehydrates to a new crystalline phase. Thus the type of the auxiliary ligands appears to be a key factor that affects the dehydration-rehydration properties of the resulting framework. To the best of our knowledge, **1** also represents the first lead(II)-organic framework that shows *in situ* rapid and reversible dehydration-rehydration behavior just in the air, so may possibly be used as potential adsorbent and sensing material to water vapor. The materials **1**, **2A**, **3** and **4** have been found to exhibit blue fluorescence in the solid state. The water

molecules in **1** and **3** have great influence on their fluorescent emission intensity. This work will give impetus to the further investigation of the coordination chemistry of $asba^{2-}$. Further work is in progress in our laboratory to prepare other novel MOFs based on the ligand $asba^{2-}$ with interesting tunable functional properties.

Experimental section

Materials and measurements

The auxiliary ligand 1,4-(methylene-benzene)bisimidazole (bix) was prepared according to the literature method.[24] The other reagents were purchased commercially and used without further purification. Elemental analyses (C, H and N) were carried out on a 240 C Elemental analyzer. FT-IR spectra (400 - 4000 cm^{-1}) were recorded from KBr pellet in a Magna 750 FT-IR spectrophotometer. Solid state fluorescent spectra were recorded using an F 4500 fluorescence spectrometer equipped with phosphorescence device. Both the excitation and emission pass width are 5.0 nm. Thermogravimetric analysis was taken on NETZSCH STA 409 PG/PC instrument from room temperature to 800 ˚C at a heating rate of 10 ˚C/min in N_2. X-ray powder diffraction data were collected on a computer controlled Bruker D8 Advanced XRD diffractometer operating with Cu-K$\alpha_{1/2}$ (λ = 1.5418 Å) radiation at a scanning rate 0.024 °/s from 5° to 20° using a VÅNTEC solid-state detector. The diffractometer was fitted with an Anton-Parr XRK900 heating stage for variable temperature studies. Thermogravimetric analysis (TGA) was taken on NETZSCH STA 409 PG/PC instrument under a stream of N_2 (10 ml/min).

Crystal structure determination

Crystallographic data for **1-4** were collected with a Siemens SMART CCD diffractormeter using graphite-monochromated (Mo-Kα) radiation (λ = 0.71073 Å), ψ and ω scans mode. The structures were solved by direct methods and refined by Full-Matrix least-squares on F^2 method using SHELXL-97 program.[25] Intensity data were corrected for Lorenz and polarization effects and a multi-scan absorption correction was performed. All non-hydrogen atoms were refined anisotropically. The carbon/nitrogen-bound hydrogen atoms of all the complexes were added geometrically and allowed to ride on their respective parent atoms. The oxygen-bound hydrogen atoms of water molecules were firstly located in the difference Fourier map and then kept fixed. The contribution of these hydrogen atoms was included in the structure factor calculations. Details of crystal data, collection and refinement are listed in Table 1.

Synthesis of $\{[Pb_2(asba)_2(phen)_2(H_2O)]\cdot 2H_2O\}_n$ (1)

A mixture of $Pb(NO_3)_2$ (0.033 g, 0.100 mmol) and phen (0.020 g, 0.100 mmol) in water (12 ml) was added to a mixture of H_2asba (0.022 g, 0.100 mmol) and NaOH (0.008 g, 0.200 mmol) in water (6 ml). The filtrate was kept at ambient temperature for several days to yield pale yellow needle-like crystals (yield: 43 mg; 69 % based on H_2asba). Anal. Calcd (%) for $C_{38}H_{32}N_6O_{13}Pb_2S_2$: C, 36.24; H, 2.56; N, 6.68. Found: C, 36.14; H, 2.45; N, 6.57. Selected IR data (KBr pellet, cm^{-1}): 3436(s), 3050(w), 1606(s), 1570(s), 1505(s), 1417(s), 1396(s), 1309(w), 1193(vs), 1128(w), 1040(s), 837(s), 722(s), 618(m).

Synthesis of $\{[Pb_2(asba)_2(bipy)_2(H_2O)]\cdot 2H_2O\}_n$ (2)

A mixture of $Pb(NO_3)_2$ (0.033 g, 0.100 mmol) and bipy (0.008 g, 0.050 mmol) in water/CH_3CH_2OH = 1:1 (6 ml) was added to a mixture of H_2asba (0.022 g, 0.100 mmol) and NaOH (0.004 g, 0.100 mmol) in water (5 ml). The filtrate was kept at ambient temperature for several days to yield pale yellow needle-like crystals. The crystal loses crystallinity in air and transforms into $\{[Pb_2(asba)_2(bipy)_2(H_2O)]\cdot H_2O\}_n$ (**2A**) (yield: 21 mg; 71 % based on bipy). Anal. Calcd (%) for $C_{34}H_{30}N_6O_{12}Pb_2S_2$: C, 34.21; H, 2.51; N, 7.03. Found: C, 34.09; H, 2.43; N, 6.89. Selected IR data (KBr pellet, cm^{-1}): 3390(s), 3312(w), 1613(s), 1563(s), 1505(s), 1439(s), 1417(s) 1374(vs) 1324(s), 1223(vs), 1148(vs), 1004(w), 830(s), 749(s), 706 (s), 648(w).

Synthesis of $[Pb_2(asba)_2(bix)_2(H_2O)_2]_n$ (3)

A mixture of H_2asba (0.011 g, 0.050 mmol) and NaOH (0.002 g, 0.050 mmol) in water (5 ml) and $Pb(NO_3)_2$ (0.033 g, 0.1 mmol) was added to a solution of bix (0.014 g, 0.050 mmol) in CH_3OH (3 ml). The filtrate was kept at ambient temperature for several days to yield pale yellow needle-like crystals (yield: 17 mg; 59 % based on H_2asba). Anal. Calcd (%) for $C_{28}H_{28}N_6O_{12}Pb_2S_2$: C: 30.05; H,2.52; N, 7.51. Found: C, 30.25; H,2.59; N, 7.41. Selected IR data (KBr pellet, cm^{-1}): 3400(s), 3066(w), 1649(s), 1584(s), 1482(vs), 1426(s), 1338(s), 1214(s), 1142(s), 1083(w), 851(vs), 752(vs), 675 (w), 605(s).

Synthesis of $[Pb(asba)(H_2O)]_n$ (4)

A mixture of H_2asba (0.011 g, 0.050 mmol) and NaOH (0.004 g, 0.100 mmol) was dissolved in water (5 ml) and then an aqueous solution of $Pb(NO_3)_2$ (0.033 g, 0.100 mmol) in water (5 ml) was added whilst stirring. The filtrate was kept at ambient

temperature for several days and pale yellow block crystals were formed (yield: 15 mg; 70 % based on H_2asba). Anal. Calc. for $C_7H_7NO_6PbS_1$: C, 19.08; H, 1.60; N, 3.18. Found: C, 18.89; H, 1.48; N, 3.06%. Selected IR data (KBr pellet, cm^{-1}): 3365 (s), 3083 (w), 1622(s), 1582(s), 1513(s), 1430(ws), 1362(vs), 1219(vs), 1115(vs), 1062(vs), 896(s), 827 (s), 793(w), 704 (s), 636(w).We found that **4** could also be obtained in the presence of bte, btp, btb, bth or bbtz with the same molar amount as H_2asba.

Supplementary material

Crystallographic data have been deposited with the Cambridge Crystallographic Data Centre with Nos. (**1**) 835434, (**2**) 834929, (**3**) 835435, (**4**) 835436 and (**H_2asba**) 989589. Copies of the data can be obtained free of charge *via* the Internet at http://www.ccdc.cam.ac.uk/conts/retrieving.html.

Acknowledgment

The Natural Science Foundation of Jiangsu Province (BK2012680) and the Priority Academic Program Development of Jiangsu Higher Education Institutions (PAPD) are gratefully acknowledged.

References

1 (*a*) G. Férey, C. Mellot-Draznieks, C. Serre, F. Millange, J. Dutour, S. Surble and I. Margiolaki, *Science* 2005, **309**, 2040; (*b*) F. Millange, C. Serre, N. Guillou, G. Férey and R. I. Walton, *Angew. Chem. Int. Ed.,* 2008, **47**, 4100; (*c*) S. Kitagawa and K. Uemura, *Chem. Soc .Re*v. 2005, **34**, 109; (*d*) J. W. Steed and J. L. Atwood, *Supramolecular Chemistry*; Wiley and Sons: New York, 2000; (*e*) S. R. Batten and R. Robson, *Angew. Chem. Int. Ed.* 1998, **37**, 1460; (*f*) G.-X. Liu, Y.-Q. Huang, Q. Chu, T. Okamura, W.-Y. Sun, H. Liang and N. Ueyama, *Cryst. Growth Des.* 2008,

8, 3233; (*g*) F.-Q. Wang, X.-J. Zheng, Y.-H. Wan, C.-Y. Sun, Z.-M. Wang, K. -Z. Wang and L. -P. Jin, *Inorg. Chem.* 2007, **46**, 2956; (*h*) G. J. Halder and C. J. Kepert, *J. Am. Chem. Soc.,* 2005, **127**, 7891; (*i*) I. Grobler, V. J. Smith, P. M. Bhatt, S. A. Herbert and L. J. Barbour *J. Am. Chem. Soc.* 2013, **135**, 6411; (*j*) L. Du, Z. Lu, K. Zheng, J. Wang, X. Zheng, Y. Pan, X. You and J. Bai, *J. Am. Chem. Soc.* 2013, **135**, 562. (*k*) D.-S. Li, Y.-P. Wu, J. Zhao, J. Zhang and J. Y. Lu *Coord. Chem. Rev*. 2014, **261**, 1.

2 (*a*) Y. Y. Niu, H. G. Zheng, H. W. Hou and X. Q. Xin, *Coord. Chem. Rev*. 2004, **248**, 169; (*b*) J. Heo, Y. M. Jeon and C. A. Mirkin, *J. Am. Chem. Soc.* 2007, **129,** 7712; (*c*) J. Luo, H. Xu, Y. Liu, Y. Zhao, L. L. Daemen, C. Brown, T. V. Timofeeva, S. Ma and H. -C. Zhou, *J. Am. Chem. Soc.,* 2008, **130 (30)**, 9626; (*d*) O. R. Evans and W. Lin, *Acc. Chem. Res.* 2002, **35**, 511; (*e*) X. H. Bu, W. Chen, S. L. Lu, R. H. Zhang, D. Z. Liao, W. M. Shionoya, M. Bu, F. Brisse and J. Ribas, *Angew. Chem., Int. Ed.* 2001, **40,** 3201; (*f*) X.-H. Zhou, Y.-H. Peng, X.-D. Du, C.-F. Wang, J.-L. Zuo and X.-Z. You, *Cryst. Growth Des.* 2009, **9**, 1028; (*g*) L. J. Murray, M. Dincã and J. R. Long, *Chem. Soc. Rev.,* 2009, **38**, 1294; (*h*) B. Moulton and M. J. Zaworotko, *Chem. Rev*. 2001, **101**, 1629; (*i*) H. Furukawa, J. Kim, N. W. Ockwig, M. O'Keeffe and O. M. Yaghi, *J. Am. Chem. Soc.,* 2008, **130(35)**, 11650; (*j*) L. Han, Y. Zhou, W.-N. Zhao, X. Li and Y.-X. Liang, *Cryst. Growth Des.* 2009, **9**, 660. (*k*) D. Liu, K. Lu, C. Poon and, W. Lin, *Inorg. Chem.* 2014, **53**, 1916.

3 (*a*) D. T. de Lill, N. S. Gunning and C. L. Cahill, *Inorg. Chem.* 2005, **44**, 258; (*b*) K. Biradha, Y. Hongo and M. Fujita, *Angew. Chem. Int. Ed.* 2000**, 39**, 3843; (*d*) X. Zhao, G. Zhu, Q. Fang, Y. Wang, F. Sun and S. Qiu, *Cryst. Growth Des.* 2009, **9**, 737; (*e*) D. N. Dybtsev, H. Chun and K. Kim, *Angew. Chem. Int. Ed* 2004, **43**, 5033; (*f*) W. G. Lu, C. Y. Su, T. B. Lu, L. Jiang and J. M. Chen, *J. Am. Chem.Soc.* 2006, **128,** 34; (*g*) M. D. Allendorf, C. A. Bauer, R. K. Bhakta and R. J. T. Houk *Chem. Soc. Rev.,* 2009, **38**, 1330.

4 (*a*) O. M. Yaghi, M. O'Keeffe, N. W. Ockwig, H. K. Chae, M. Eddaoudi and J. Kim, *Nature* 2003, **423,** 705; (*b*) S. Kitagawa, R. Kitaura and S. I. Noro, *Angew. Chem., Int. Ed.* 2004,**43,** 2334; (*c*) C. N. R. Rao, S. Natarajan and R. Vaidhyanathan,

Angew.Chem., Int. Ed. 2004, **43,** 1466; (*d*) B. H. Ye, M. L. Tong and X. M. Chen, *Coord. Chem. Rev*. 2005, **249**, 545.

5 (*a*) I. V. Mitchell, *Pillared Layered Structures: Current Trends and Applications*; Elsevier, London, 1990; (*b*) K. T. Holman, A. M. Pivowar, J. V. Swift and M. D. Ward, *Acc. Chem. Res.* 2001, **34,** 107; (*c*) J. L. Song, H. H. Zhao, J. G. Mao and K. R. Dunbar, *Chem. Mater.* 2004, **16,** 1884; (*d*) B. Y. Lou, F. L. Jiang, B. L. Wu, D. Q. Yuan and M. C. Hong, *Cryst. Growth Des.* 2006, **6,** 989.

6 (*a*) A.M. Beatty, *Coord. Chem. Rev.*, 2003, **246,** 131; (*b*) X.-P. Li, J.-Y. Zhang, M. Pan, S.-R. Zheng, Y. Liu and C.-Y. Su, *Inorg. Chem.,* 2007, **46**, 4617.

7 (*a*) A. Strasser, and A. Vogler, *J. Photochem. Photobiol. A*, 2004, 165, 115. (*b*) A. Vogler and H. Nikol, *Pure Appl. Chem*. 1992, 64, 1311. 20.

8 (*a*) J. Yang, J. F. Ma, Y. Y. Liu, J. C. Ma and S. R. Batten, *Inorg. Chem*. 2007, **46**, 6542; (*b*) S. R. Fan and L. G. Zhu, *Inorg. Chem*. 2007, **46**, 6785; (*c*) Y. H. Zhao, H. B. Xu, Y. M. Fu, K. Z. Shao, S. Y. Yang, Z. M. Su, X. R. Hao, D. X. Zhu and E. B. Wang, *Cryst. Growth Des*. 2008, **8**, 3566; (*d*) J. Yang, J. F. Ma, Y. Y. Liu, J. C. Ma and S. R. Batten, *Cryst. Growth Des*. 2009, **9**, 1894; (*e*) J. Yang, G. D. Li, J. J. Cao, Q. Yue, G. H. Li and J. S. Chen, *Chem.-Eur. J.* 2007, **13**, 3248. (*f*) L. Shimoni-Livny, J. P. Glusker and C. W. Bock, *Inorg. Chem.* 1998, **37**, 1853.

9 (*a*) M. J. Katz, P. M. Aguiar, R. J. Batchelor, A. A. Bokov, Z.-G. Ye, S. Kroeker, and D. B. Leznoff, *J. Am. Chem. Soc.*, 2006, **128(11)**, 3669; (*b*) F. Bonhomme, T. M. Alam, A. J. Celestian, D. R. Tallant, T. J. Boyle, B. R. Cherry, R. G. Tissot, M. A. Rodriguez, J. B. Parise and M. Nyman, *Inorg. Chem*. 2005, **44**, 7394; (*c*) S.-R. Fan and L.-G. Zhu, *Inorg. Chem*. 2006, **45**, 7935; (*d*) R. Sasai and H. Shinomura *J. Solid State Chem.*, 2013, **198**, 452; (*e*) S. H. Deo, and A. Godwin, *J. Am. Chem. Soc*. 2000, **122**, 174; (*f*) J. Li and Y. Lu, *J. Am. Chem. Soc*. 2000, **122**, 10466; (*g*) M. H. Jack, M. Saeed and A. S. Ali, *Inorg. Chem*. 2004, **43**, 1810; (*h*) L. K. Li, Y. L. Song, H. W. Hou, Y. T. Fan and Y. Zhu, *Eur. J. Inorg. Chem*. 2005, 3238; (*i*) X.-Y. Yu, R. Xin, W.-P. Gao, N. Wang, X. Zhang, Y.-Y. Yang and X.-S. Qu, *J. Solid State Chem.*, 2013, **204**, 314; (*j*) Y. H. Yeom, Y. Kim and K. Seff, *Microporous Mesoporous Mater.* 1999, **28**, 103; (*k*) Y. H. Yeom, Y. Kim and K. Seff, *J. Phys.*

Chem., 1997, **B101**, 5314; (*l*) F. Frostemark, L. A. Bengtsson and B. Holmberg, *J. Chem. Soc. Faraday Trans.* 1994, **90**, 2531. (*m*) L. Li, S. Q. Zhang, L. Han, Z. H. Sun, J. H. Luo and M. C. Hong, *Cryst. Growth Des.* 2013, **13**, 106. (*n*) D.-S. Li, Y.-P. Wu, P. Zhang, M. Du, J. Zhao, C.-P. Li and Y.-Y. Wang *Cryst. Growth Des*. 2010, **10**, 2037; (*o*) X.-M. Lin, T.-T. Li, L.-F. Chen, L. Zhang and C.-Y. Su, *Dalton Trans.*, 2012, **41**, 10422.

10 (*a*) F. J. M. Casado, L. Cañadillas-Delgado, F. Cucinotta, A. Guerrero-Martínez, M. R. Riesco, L. Marchese and J. A. R. Cheda, *CrystEngComm*, 2012, **14**, 2660; (*b*) Y.-H. Zhao, H.-B. Xu, K.-Z. Shao, Y. Xing, Z.-M. Su and J.-F. Ma, *Cryst. Growth Des*. 2007, **7**, 513; (*c*) K.-L. Zhang, F. Zhou, R. Wu, B. Yang and S. W. Ng, *Inorg. Chim. Acta* 2009, **362**, 4255; (*d*) K. -L. Zhang, Y. Chang, C. T. Hou, R. Wu, G. W. Diao and S. W. Ng, *CrystEngComm* 2010, **12**, 1194; (*e*) K. -L. Zhang, Z. -C. Pan, W. Liang, W. -L Liu and S. W. Ng, *Mater. Lett.* 2009, **63**, 2136; (*f*) K. -L. Zhang, Y. Chang, J. -B. Zhang, Y. Deng, T. -T. Qiu, L. Li and S. W. Ng, *CrystEngComm*, 2012, **14**, 2926.

11 (*a*) M. J. Katz, P. M. Aguiar, R. J. Batchelor, A. A. Bokov, Z.-G. Ye, S. Kroeker, and D. B. Leznoff, *J. Am. Chem. Soc.* 2006, **128**, 3669; (*b*) M. J. Katz, H. Kaluarachi, R. J. Batchelor, A. A. Bokov, Z. -G. Ye and D. B. Leznoff, *Angew. Chem., Int. Ed.* 2007, **46**, 8804.

12 (*a*) K. P. Rao and A. Thirumurugan and C. N. R. Rao, *Chem.-Eur. J.* 2007, **13**, 3193; (*b*) A. Thirumurugan, R. A. Sanguramath and C. N. R. Rao, *Inorg. Chem.* 2008, **47**, 823.

13 (*a*) M.A.R. Dakers, M.N.S. Hill, J.C. Lockhart and D.J. Rushton, *J. Chem. Soc., Dalton Trans.*, 1994, 209; (*b*) P. Schwerdtheger, G.A. Heath, M. Dolg and M.A. Bennett, *J. Am. Chem. Soc.,* 1992, **114**, 7518; (*c*) K. Byriel, K.R. Dunster, L.R. Gahan, C.H.L. Kennard, J.L. Latten, I.L. Swann, P.A. Duckworth, *Polyhedron*, 1992, **11**, 1205; (*d*) P. Pyykko, *Chem. Rev.*, 1988, **88**, 563.

14 (*a*) A. Bashall, M. Mcpartlin, B.P. Murphy, D.E. Fenton, S.J. Kitchen and P.A. Tasker, *J. Chem. Soc., Dalton Trans.,* 1990, 505; (*b*) A.K. Cheetham, G. Férey and T. Loiseau, *Angew. Chem. Int. Ed.,* 1999, **38**, 3268; (*c*) N. Stock, S.A. Férey, G.D. Stucky and A.K. Cheetham, *J. Chem. Soc., Dalton Trans.*, 2000, 4292; (*d*) X.

Luo, L. Liu, F. Deng and S. Luo, *J. Mater. Chem. A*, 2013, **1**, 8280.

15 (*a*) V. Safarifard, A. Morsali, S. W. Joo, *Ultrason. Sonochem.* 2013, **20**, 1254; (*b*) M. L. Hu, A. Morsali and L. Aboutorabi, *Coord. Chem. Rev.* 2011, **255**, 2821; (*c*) O. Sadeghzadeh, A. Morsali, V. T. Yilmaz and O. Büyükgüngör, *Inorg. Chim. Acta*. 2010, **363**, 841; (*d*) F. Fredoueil, M. Evain, D. Massiot, M. Bujoli-Doeuff, P. Janvier, A. Clearfield and B. Bujoli, *J. Chem. Soc., Dalton Trans.*, 2002, 1508; (*e*) B. Chen, S. Ma, F. Zapata, F. R. Fronczek, E. B. Lobkovsky and H.-C. Zhou, *Inorg. Chem.* 2007, **46**, 1233.

16 (*a*) S. R. Batten, S. M. Neville and D. R. Turner, *Coordination Polymers: Design, Analysis and Applications*; RSC Publishing: Cambridge, 2009; (*b*) W. L. Leong and J. J. Vittal, *Chem. Rev*. 2011, **111**, 688; (*c*) P. Diaz, J. Benet-Buchholz, R. Vilar and A. J. P. White, *Inorg. Chem*. 2006, **45**, 1617; (*d*) K. -L. Zhang, C. T. Hou, J.-J. Song, Y. Deng, L. Li, S. W. Ng and G.-W. Diao, *CrystEngComm*, 2012, **14**, 590. (*e*) C. Gabriel, M. Perikli, C. P. Raptopoulou and A. Terzis, *Inorg. Chem.* 2012, **51**, 9282.

17 (*a*) K. M. Guckian, B. A. Schweitzer, R. X.-F. Ren, C. J. Sheils, D. C. Tahmassebi and E. T. Kool, *J. Am. Chem. Soc.,* 2000, **122**, 2213; (*b*) Y. Kim, J. H. Geiger, S. Hahn and P. B. Sigler, *Nature,* 1993, **365,** 512; (*c*) J. L. Kim, D. B. Nikolov and S. K. Burley, *Nature,* 1993, **365**, 520; (*d*) C. A. Hunter and J. K. M. Sanders, *J. Am. Chem. Soc.,* 1990, **112**, 5525.

18 (*a*) M. Arfa, R. Olier and M. Privat *J. Phys. Chem. A* 2008**, 112***,* 6004; (*b*) C. Gourlaouen and O. Parisel. *Angew. Chem., Int. Ed*., 2007, **46**, 553; (*d*) R. D. Hancock, J. H. Reibenspies and H. Maumela. *Inorg. Chem*., 2004, **43**, 2981. (*e*) V. Mah and F. Jalilehvand, *Inorg. Chem.* 2012, **51**, 6285.

19 R. D. Hancock, M. S. Shaikjee, S. M. Dobson and J. C. A. Boeyens, *Inorg. Chim. Acta*., 1988, **154**, 229.

20 D. Eisenberg and W. Kauzmann, *The Structure and Properties of Water*; Oxford University Press: Oxford, 1969.

21 K. Nakamoto, *Infrared and Raman Spectra of Inorganic and Coordination Compounds*, 4th edn., Wiley, New York, 1986, 231.

22 S. Coriani, A. Halkier, A. Rizzo and K. Ruud, *Chem. Phys. Lett.*, 2000, **326**, 269.

23 (*a*) A. Vogler and H. Kunkely, *Coord. Chem. Re*v. 2007, **251**, 577; (*b*) D. Rendell *Fluorescence and Phosphorescence*. New York: John Willey & Sons, 1987; (c) P.C. Ford and A. Vogler, *Acc. Chem. Res*. 1993, **26**, 220; (d) A. Vogler, A. Paukner and H. Kunkely, *Coord. Chem. Re*v.1980, **33**, 227.

24 B. F. Hoskins, R. Robson and D. A. Slizys *J. Am. Chem. Soc.* 1997**, 119***,* 2952.

25 G.M. Sheldrick, SHELXL 97. *Programs for Crystal Structure Analysis* (Release 97-2), 1997, University of Götinggen, Germany.

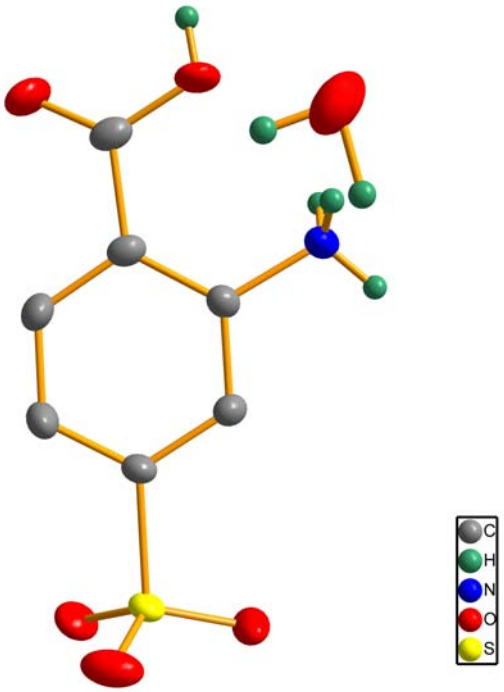

Chart 1 Molecular structure of H_2asba·H_2O with 50 % ellipsoids.

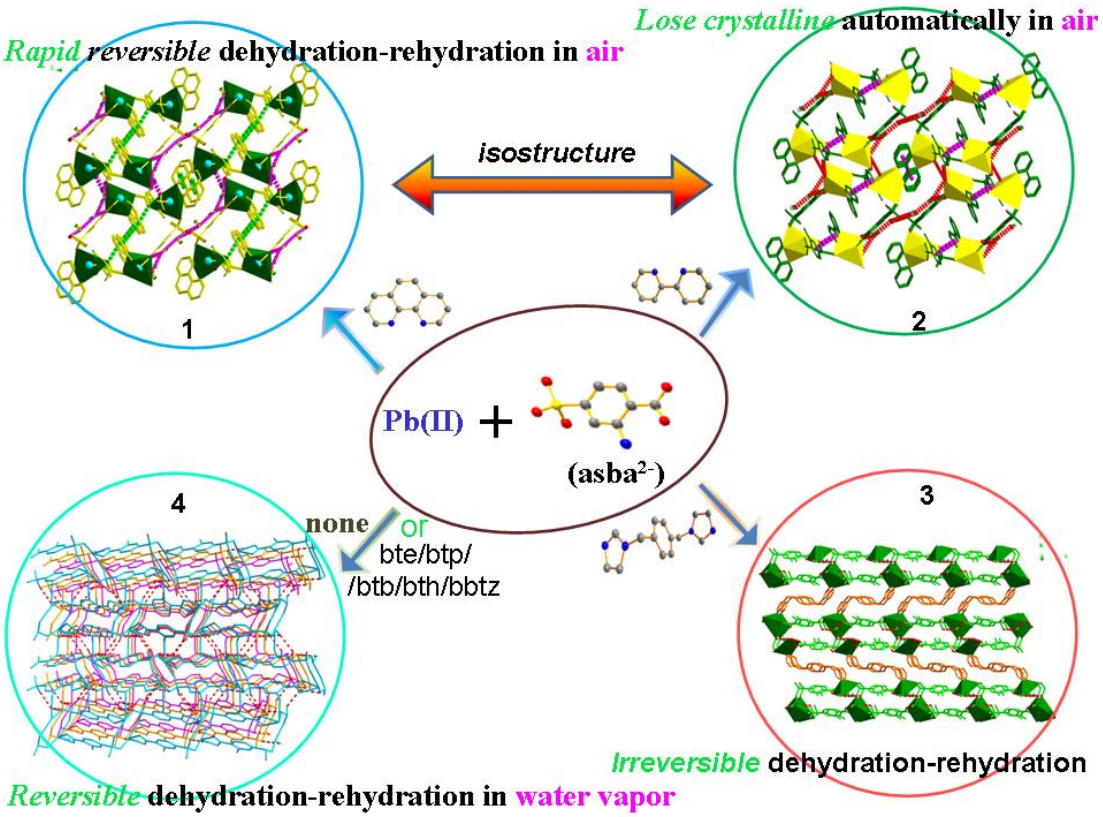

Scheme 1. Simplified representation of the synthesis and crystalline architectures of 1-4 as well as showing the rich auxiliary ligand-dependent dehydration-rehydration behaviours of these four MOFs.

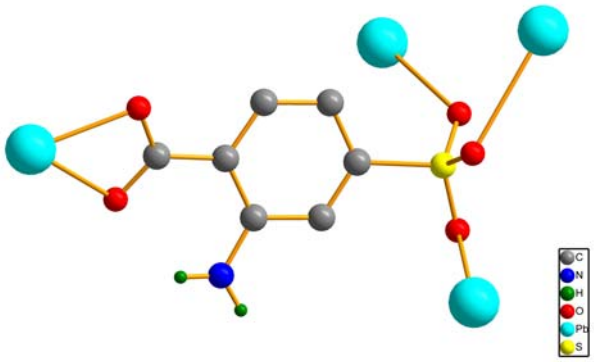

η^1:η^1:η^1:η^1:η^1:μ_4- in **1** and **2**

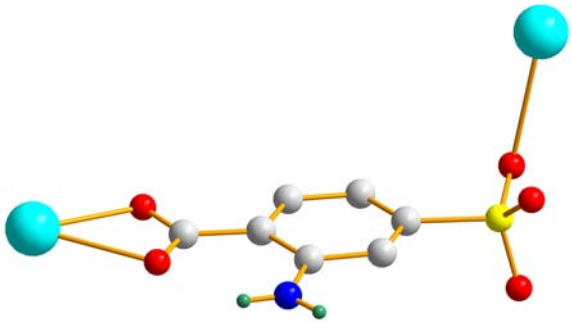

η^1:η^1:η^1:μ_2- in **1** and **2**

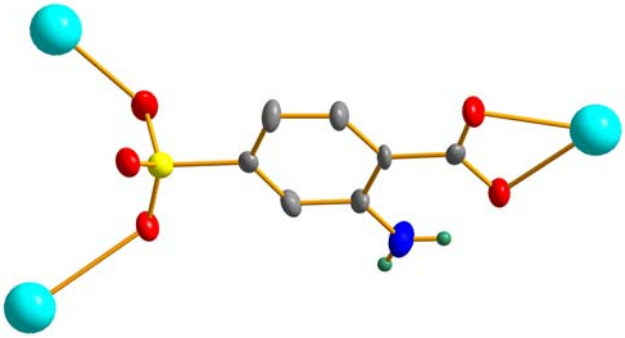

η^1:η^1:η^1:η^1:μ_3- in **3**

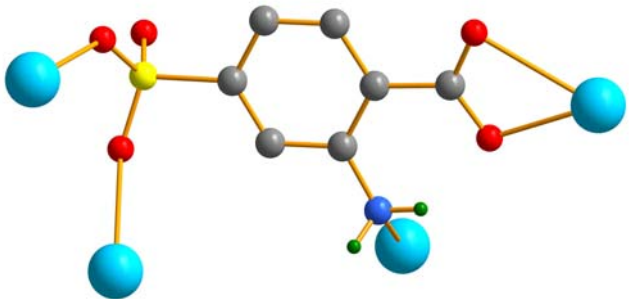

η^1:η^1:η^1:η^1:η^1:μ_4- in **4**

Scheme 2. Simplified representation of the coordination modes of asba^{2-} in 1-4.

Table 1. Crystallographic data and structure refinement details for **1-4**.

Complex	**1**	**2**	**3**	**4**
Empirical formula	$C_{38}H_{32}N_6O_{13}Pb_2S_2$	$C_{34}H_{32}N_6O_{13}Pb_2S_2$	$C_{28}H_{28}N_6O_{12}$ Pb_2S_2	$C_7H_7NO_6PbS$
Formula weight	1259.20	1211.20	1119.06	440.39
Temperature	296(2)	296(2)	296(2)	296(2)
Wavelength/ Å	0.71073	0.71073	0.71073	0.71073
Crystal system	Triclinic	Triclinic	Triclinic	Monoclinic
Space group	*P-1*	*P-1*	*P-1*	$P2_1/c$
a/Å	9.6177(15)	9.7272(10)	5.9314(7)	6.6780(11)
b/Å	13.490(2)	13.4690(14)	11.0291(13)	14.672(3)
c/Å	15.996(2)	15.4478(16)	24.939(3)	9.7183(17)
α/°	90.087(2)	89.2900(10)	101.0520(10)	90□
β/°	96.643(2)	83.6170(10)	92.705(2)	95.169
γ/°	105.861(2)	70.4760(10)	93.508(2)	90
V/ Å^3	1981.8(5)	1895.0(3)	1595.3(3)	948.3(3)
Z	2	1	2	4
D_c / Mg m^{-3}	2.110	2.123	2.330	3.084
Absorption coeff /mm^{-1}	8.665	9.057	10.745	18.024
F(000)	1204	1156	1060	808
*θ r*ange for data collection /°	1.28 to 27.58	1.60 to 27.56	1.67 to 27.48 .	2.52 to 27.55 .
Index ranges	-12≤*h*≤12, -17≤*k*≤17, -20≤*l*≤20	-12≤*h*≤12, -17≤*k*≤17, -17≤*l*≤20	-7≤*h*≤7, -14≤*k*≤14, -32≤*l*≤30	-8≤*h*≤8, -18≤*k*≤19, -12≤*l*≤11
Reflections collected	17376	16657	14086	8085
Unique(R_{int})	8952 [*R*(int) = 0.0432]	8555 [*R*(int) = 0.0504]	7182 [*R*(int) = 0.0436]	2177 [*R*(int) = 0.0450]
Completeness	97.5 %	97.8 %	97.9 %	99.8 %
Max. and min. transmission	0.3564and0.1514	0.404 and 0.154	0.2956and0.1169	0.067 and 0.019
Goof on F^2	1.010	1.079	1.062	1.091
Final *R* indices [*I*>2σ(*I*)]	R_1 = 0.0437, wR_2 = 0.1038	R_1 = 0.0419, wR_2 = 0.1175	R_1 = 0.0394, wR_2 = 0.0963	R_1 = 0.0263, wR_2 = 0.0688
R indices (all data)	R_1 = 0.0799, wR_2 = 0.1297	R_1=0.0545, wR_2 = 0.1294	R_1 = 0.0527, *w*R2 = 0.1085	R_1 = 0.0292, wR_2 = 0.0705
Largest diff. Peak and hole / e Å^{-3}	1.842 and -1.166	1.634 and -2.285	1.826 and -1.643	2.252 and -1.446

Table 2. Selected bond lengths [Å] and angles [°] for 1-4.

Complex 1			
Pb(1)-N(3)	2.623(8)	Pb(1)-O(1)	2.455(6)
Pb(1)-N(2)	2.591(7)	Pb(1)-O(2)	2.526(6)
Pb(1)-O(1W)	2.754(8)	Pb(1)-O(5)#2	2.914(7)
Pb(1)-O(6)#1	2.799(7)	Pb(2)-O(4)	2.759(7)
Pb(2)-N(5)	2.497(7)	Pb(2)-O(6)	2.455(6)
Pb(2)-N(6)	2.597(8)	Pb(2)-O(8)	2.394(6)
Pb(2)-O(7)	2.844(6)		
O(1)-Pb(1)-O(2)	52.4(2)	O(3)-Pb(2)-C(20)	105.6(2)
O(1)-Pb(1)-N(2)	76.1(2)	O(7)-Pb(2)-N(4)	76.3(2)
O(2)-Pb(1)-N(2)	79.2(2)	O(6)-Pb(2)-N(4)	121.9(2)
O(1)-Pb(1)-N(1)	93.0(2)	N(3)-Pb(2)-N(4)	65.0(3)
O(2)-Pb(1)-N(1)	135.3(2)	O(7)-Pb(2)-O(3)	131.2(2)
N(2)-Pb(1)-N(1)	63.7(2)	O(6)-Pb(2)-O(3)	80.5(2)
O(1)-Pb(1)-O(1W)	72.9(2)	N(3)-Pb(2)-O(3)	73.8(2)
O(2)-Pb(1)-O(1W)	114.7(2)	N(4)-Pb(2)-O(3)	124.3(2)
N(2)-Pb(1)-O(1W)	122.5(2)	O(7)-Pb(2)-C(20)	27.0(2)
N(1)-Pb(1)-O(1W)	70.9(2)	O(6)-Pb(2)-C(20)	26.8(2)
O(7)-Pb(2)-O(6)	53.8(2)	N(3)-Pb(2)-C(20)	75.7(3)
O(7)-Pb(2)-N(3)	79.3(2)	N(4)-Pb(2)-C(20)	99.0(3)
O(6)-Pb(2)-N(3)	77.1(2)		
Complex 2			
Pb(1)-N(2)	2.587(6)	Pb(2)-N(6)	2.576(6)
Pb(1)-O(1)#4	2.424(5)	Pb(2)-O(3W)	2.846(6)
Pb(1)-O(2)#4	2.446(5)	Pb(2)-O(3)	2.965(7)
Pb(1)-O(6)	2.713(6)	Pb(2)-O(10)#5	2.482(5)
Pb(1)-N(3)	2.529(6)	Pb(2)-O(9)#5	2.475(5)
Pb(1)-O(4)	2.828(5)	Pb(2)-O(5)#3	2.776(5)
Pb(2)-N(5)	2.635(7)		
O(1)#4-Pb(1)-O(2)#4	53.83(17)	O(9)#5-Pb(2)-N(5)	91.1(2)
O(1)#4-Pb(1)-N(3)	76.79(19)	O(10)#5-Pb(2)-N(5)	134.7(2)
O(2)#4-Pb(1)-N(3)	80.82(19)	N(6)-Pb(2)-N(5)	62.6(2)
O(1)#4-Pb(1)-N(2)	120.2(2)	O(9)#5-Pb(2)-O(5)#3	122.30(17)
O(2)#4-Pb(1)-N(2)	76.24(19)	O(10)#5-Pb(2)-O(5)#3	73.80(17)
N(3)-Pb(1)-N(2)	63.5(2)	N(6)-Pb(2)-O(5)#3	77.89(19)
O(1)#4-Pb(1)-O(6)	77.84(17)	N(5)-Pb(2)-O(5)#3	118.70(18)
O(2)#4-Pb(1)-O(6)	130.16(16)	O(9)#5-Pb(2)-O(3W)	74.53(18)
N(3)-Pb(1)-O(6)	76.63(19)	O(10)#5-Pb(2)-O(3W)	113.74(18)
N(2)-Pb(1)-O(6)	127.97(19)	N(6)-Pb(2)-O(3W)	123.80(19)

O(1)#4-Pb(1)-O(4)	83.68(17)	N(5)-Pb(2)-O(3W)	72.40(19)
O(2)#4-Pb(1)-O(4)	79.87(17)	O(5)#3-Pb(2)-O(3W)	157.24(18)
N(3)-Pb(1)-O(4)	158.21(17)	O(9)#5-Pb(2)-O(10)#5	52.42(18)
N(2)-Pb(1)-O(4)	120.8(2)	O(9)#5-Pb(2)-N(6)	74.5(2)
O(6)-Pb(1)-O(4)	108.82(16)	O(10)#5-Pb(2)-N(6)	80.4(2)
O(9)#5-Pb(2)-O(3)	88.53(18)	N(5)-Pb(2)-O(3)	132.67(19)
O(10)#5-Pb(2)-O(3)	78.40(18)	O(5)#3-Pb(2)-O(3)	100.82(16)
N(6)-Pb(2)-O(3)	158.23(17)	O(3W)-Pb(2)-O(3)	61.96(16)
Complex 3			
Pb(1)-O(6)	2.758(6)	Pb(2)-N(2)	2.466(7)
Pb(1)-N(5)	2.422(7)	Pb(2)-O(4)	2.647(6)
Pb(1)-O(8)#1	2.947(6)	Pb(2)-O(5)	2.468(6)
Pb(1)-O(2W)	2.428(6)	Pb(2)-O(1)	2.954(7)
Pb(1)-O(7)	2.400(6)	Pb(2)-O(9)#1	2.805(8)
Pb(2)-O(2)#2	2.873(5)	Pb(2)-O(1W)	2.531(5)
N(5)-Pb(1)-O(2W)	90.8(2)	N(2)-Pb(2)-O(5)	79.4(2)
O(7)-Pb(1)-O(6)	49.8(2)	N(2)-Pb(2)-O(1W)	90.7(2)
O(7)-Pb(1)-N(5)	79.2(2)	O(5)-Pb(2)-O(1W)	69.01(18)
O(7)-Pb(1)-O(2W)	69.9(2)	N(2)-Pb(2)-O(4)	77.8(2)
N(5)-Pb(1)-O(6)	75.8(2)	O(5)-Pb(2)-O(4)	51.02(18)
O(2W)-Pb(1)-O(6)	119.5(2)	O(1W)-Pb(2)-O(4)	119.99(18)
Complex 4			
Pb(1)-O(1W)	2.485(3)	Pb(1)-O(5)#4	2.358(3)
Pb(1)-O(3)	2.754(3)	Pb(1)-O(2)#2	2.629(3)
Pb(1)-N(1)#5	2.767(5)	Pb(1)-O(4)#4	2.713(4)
O(5)#4-Pb(1)-O(1W)	70.28(12)	O(2)#2-Pb(1)-O(3)	134.91(10)
O(5)#4-Pb(1)-O(2)#2	79.73(11)	O(4)#4-Pb(1)-O(3)	66.74(11)
O(1W)-Pb(1)-O(2)#2	75.16(11)	O(5)#4-Pb(1)-N(1)#5	75.37(11)
O(5)#4-Pb(1)-O(4)#4	50.90(11)	O(1W)-Pb(1)-N(1)#5	72.02(11)
O(1W)-Pb(1)-O(4)#4	116.73(11)	O(2)#2-Pb(1)-N(1)#5	143.86(10)
O(2)#2-Pb(1)-O(4)#4	73.72(11)	O(4)#4-Pb(1)-N(1)#5	108.33(11)
O(5)#4-Pb(1)-O(3)	91.23(11)	O(3)-Pb(1)-N(1)#5	71.85(10)
O(1W)-Pb(1)-O(3)	142.52(12)		

Symmetry transformations: #1 1-x 1-y 1-z #2 x-1 y-1 z for **1**; #2 x,y+1,z #3 -x+1,-y+1,-z #4 x+1,y,z #5 x,y-1,z for **2**; # 1 -x, 1-y, z #2 x-1, y-1, z for **3**; #2 -x,-y+1,-z+2 #4 x,y,z+1 #5 x,-y+1/2,z+1/2 for **4**.

Table 3 Hydrogen bonds for 1-4.

D-H...A	d(D-H)	d(H...A)	d(D...A)	<DHA	Symmetry of A
Complex 1					
O1W -- H1WA ...O2W	0.8500	2.0600	2.887(10)	164.00	
N1 -- H1A ... O2	0.8600	2.0600	2.686(11)	129.00	
N1 -- H1B ... O2W	0.8600	2.3600	3.165(12)	155.00	-1+x,y,z
O2W -- H2WA ... O3W	0.8500	2.0300	2.838(12)	158.00	
O2W -- H2WB ... O1	0.8500	2.0400	2.806(11)	149.00	
N4 -- H4A ... O9	0.8600	2.1100	2.729(11)	128.00	
N4 -- H4B ... O10	0.8600	2.3600	3.081(12)	142.00	1+x,y,z
O3W -- H3WB ...O3	0.8500	2.1200	2.886(12)	149.00	-x,1-y,-z
O1W -- H1WB ... O8	0.8500	1.9400	2.785(9)	169.00	x,-1+y,z
Complex 2					
O1W -- H1WA ... O9	0.8500	1.9800	2.764(9)	152.00	x,-1+y,z
N1 -- H1A ... O2W	0.8600	2.5200	3.189(11)	135.00	-1+x,1+y,z
N1 -- H1A ... O8	0.8600	2.5800	3.326(11	145.00	
N1 -- H1B ... O1	0.8600	2.0700	2.700(10)	129.00	
O1W -- H1WB ... O2W	0.8500	1.9900	2.824(9)	167.00	
O2W -- H2WB ... O7	0.8500	2.3700	3.160(9)	155.00	1+x,-1+y,z
O2W -- H2WA ... O7	0.8500	2.1500	2.892(9)	146.00	1-x,1-y,1-z
N4 -- H4B ... O10	0.8600	2.0400	2.680(10)	130.00	
O3W -- H3WB ... O2	0.8500	2.1000	2.901(8)	158.00	1+x,y,z
O3W -- H3WA ... O1W	0.8500	2.0300	2.806(9)	152.00	
Complex 3					
O1W -- H1WA ...O4	0.8500	1.9600	2.773(8)	158.00	-1+x,y,z
O1W -- H1WB ... O3	0.8500	1.9600	2.770(8)	158.00	-1+x,-1+y,z
O2W -- H2WA ... O6	0.8500	1.9100	2.744(9)	164.00	-1+x,y,z
N3 -- H3B ... O4	0.8600	2.1100	2.737(10)	130.00	
O2W -- H2WB ... O9	0.8500	2.0600	2.720(9)	134.00	-1+x,-1+y,z
N6 -- H6A ... O3	0.8600	2.3200	3.167(10)	170.00	-1+x,y,z
N6 -- H6B ... O7	0.8600	2.0100	2.644(11)	130.00	
Complex 4					
O1W -- H1WB ... O3	0.8500	2.3900	2.949(5)	124.00	1+x,y,z
O1W -- H1WB ... O4	0.8500	2.2100	2.998(5)	154.00	1+x,y,1+z
N1 -- H1A ... O1	0.9000	2.4500	3.299(5)	157.00	1+x,y,z
N1 -- H1B ... O5	0.9000	1.9700	2.718(5)	139.00	
O1W -- H1WA ... O1	0.8500	1.9900	2.771(5)	152.00	1+x,1/2-y,1/2+z

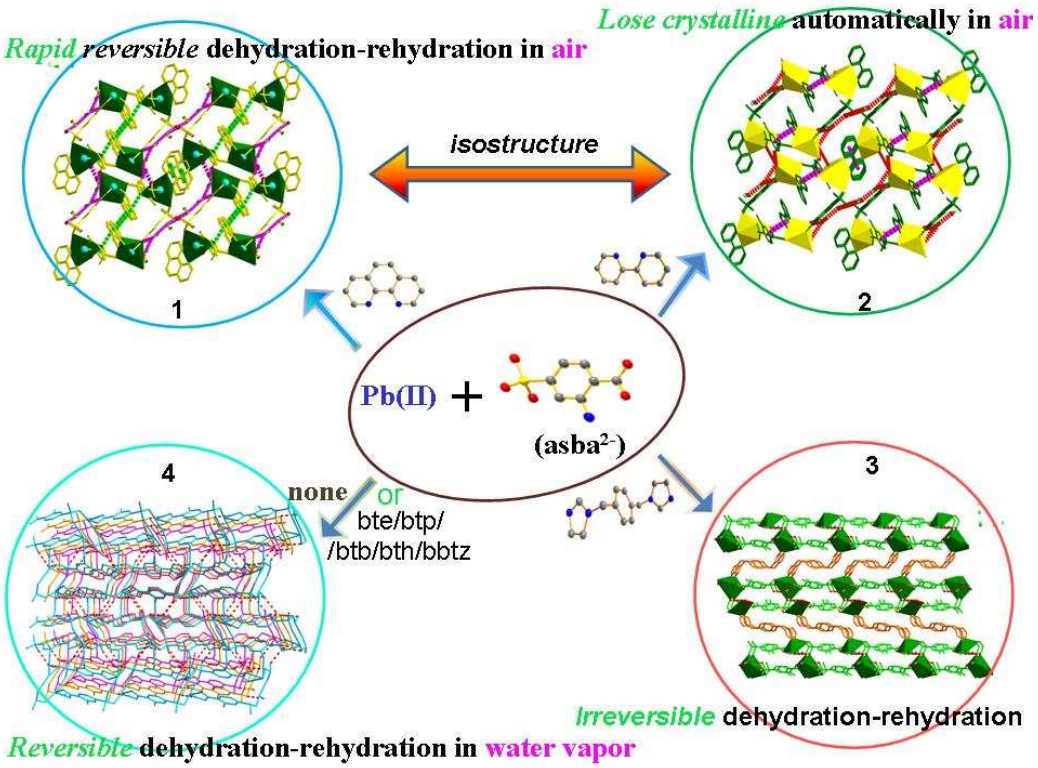

Simplified representation of the architectures and auxiliary ligand-dependent dehydration-rehydration behaviours of 1-4.